doi:10.1093/plphys/kiaa071 PLANT PHYSIOLOGY 2021: 185: 796–814

Plant Physiology

Research Article

Large fluxes of fatty acids from membranes to triacylglycerol and back during N-deprivation and recovery in *Chlamydomonas*

Danielle Yvonne Young [1] **and Yair Shachar-Hill** [1,*,†]

1 Department of Plant Biology, Michigan State University, East Lansing, Michigan, 48824, USA

*Author for communication: yairhill@msu.edu
†Senior author.

D.Y.Y. codesigned the research, performed the experiments, analyzed data, and co-wrote the manuscript. Y.S.-H. codesigned the research, interpreted results, and co-wrote the manuscript.

The authors responsible for distribution of materials integral to the findings presented in this article in accordance with the policy described in the Instruction for Authors (https://academic.oup.com/plphys) is: Yair Shachar-Hill (yairhill@msu.edu)

Abstract

Microalgae accumulate triacylglycerol (TAG) during nutrient deprivation and break it down after nutrient resupply, and these processes involve dramatic shifts in cellular carbon allocation. Due to the importance of algae in the global carbon cycle, and the potential of algal lipids as feedstock for chemical and fuel production, these processes are of both ecophysiological and biotechnological importance. However, the metabolism of TAG is not well understood, particularly the contributions of fatty acids (FAs) from different membrane lipids to TAG accumulation and the fate of TAG FAs during degradation. Here, we used isotopic labeling time course experiments on *Chlamydomonas reinhardtii* to track FA synthesis and transfer between lipid pools during nitrogen (N)-deprivation and resupply. When cells were labeled before N-deprivation, total levels of label in cellular FAs were unchanged during subsequent N-deprivation and later resupply, despite large fluxes into and out of TAG and membrane lipid pools. Detailed analyses of FA levels and labeling revealed that about one-third of acyl chains accumulating in TAG during N-deprivation derive from preexisting membrane lipids, and in total, at least 45% of TAG FAs passed through membrane lipids at one point. Notably, most acyl chains in membrane lipids during recovery after N-resupply come from TAG. Fluxes of polyunsaturated FAs from plastidic membranes into TAG during N-deprivation were particularly noteworthy. These findings demonstrate a high degree of integration of TAG and membrane lipid metabolism and highlight a role for TAG in storage and supply of membrane lipid components.

Introduction

As the supply of petroleum fuels is finite and the effects of global climate change become more pronounced (Höök and Tang, 2013), interest in renewable, carbon-neutral sources of feedstocks for bioenergy, and chemical production has increased. Microalgae have drawn attention both due to their substantial role in the carbon cycle and as attractive potential sources of feedstocks. The advantages of microalgae include their high rate of biomass production, lack of competition with food crops, higher lipid productivities per ground area than traditional crops, and their ability to accumulate a high percentage of their dry weight as triacylglycerol (TAG) under adverse environmental conditions such as nutrient deprivation (Chisti, 2007; Hu et al., 2008;

Received October 7, 2020. Accepted November 23, 2020. Advance access publication December 18, 2020

Hannon et al., 2010). TAG is a highly desirable compound, because it can be easily converted to biodiesel fuel via transesterification of its fatty acids (FAs; Durrett et al., 2008).

The unicellular green microalga *Chlamydomonas reinhardtii* has long served as a model organism for multiple cellular functions including photosynthesis, flagellar structure and function, chloroplast biogenesis, light perception, and cell cycle control (Harris, 2001; Sasso et al., 2018). The well-understood physiology of the organism (Harris, 2009), its fully sequenced genome (Merchant et al., 2007), its ability to be grown autotrophically, mixotrophically, and heterotrophically, the availability of numerous molecular tools (Jinkerson and Jonikas, 2015; Mussgnug, 2015), and its accumulation of TAG under a range of environmental stresses make *C. reinhardtii* an excellent model for investigating algal bioenergy capture and lipid metabolism (Moellering et al., 2009; Scranton et al., 2015). Nitrogen (N)-deprivation is the most widely studied inducer of TAG synthesis, as N availability is easily manipulated and induces TAG accumulation more strongly than other changes studied, while N-resupply induces a coordinated degradation of TAG and resumption of cellular growth. TAG accumulates primarily in extraplastidic oil bodies, although lipid droplets have been reported to accumulate in the chloroplast in starchless mutants under N-deprivation (Goodson et al., 2011) and in wild-type cells under high light stress (Goold et al., 2016). However, another study used electron microscopy and confocal 3D image reconstruction under a variety of conditions and found no evidence of lipid droplets in the chloroplast, rather they were exclusively found in the cytosol, although they did observe that some lipid droplets were closely associated with the chloroplast (Moriyama et al., 2018). We take these findings to mean that TAG accumulation occurs primarily in the cytosol during N-deprivation in *C. reinhardtii*.

The induction of TAG accumulation in microalgae following N-deprivation involves extensive FA synthesis and some contribution from preexisting FAs. The importance of FA synthesis is illustrated by the effect of the FA synthesis inhibitor cerulenin, which reduces TAG accumulation in *C. reinhardtii* by 80%, suggesting that FA synthesis accounts for the large majority of TAG accumulation (Fan et al., 2011). Likewise, the availability of exogenous carbon for FA synthesis during N-starvation has been reported to limit TAG accumulation (Goodson et al., 2011). Transcript analyses have provided evidence for a contribution of preexisting FAs to TAG accumulation. Schmollinger et al. (2014) found that expression of key FA synthesis genes fell early in N-deprivation and recovered after 12–24 h, suggesting that FA synthesis may contribute less to initial TAG synthesis. Other studies reported the upregulation of a large number of lipase genes during N-deprivation (Miller et al., 2010; Gargouri et al., 2015), suggesting that acyl chains may be released from existing membrane lipids, which would then be available for TAG synthesis. One such lipase, plastid galactoglycerolipid degradation 1 (PGD1), is capable of hydrolyzing 18:1Δ9 (in this work, FAs are designated as chain length:number of double bonds, with positions of double bonds indicated by Δ counting from the carboxyl group) from the *sn*-1 position of monogalactosyldiacylglycerol (MGDG), after which the FA is incorporated into TAG (Li et al., 2012a). Since 18:1Δ9 is desaturated quite rapidly after its incorporation into MGDG (Giroud and Eichenberger, 1989), PGD1 makes newly synthesized 18:1Δ9 available for TAG synthesis. Newly synthesized or preexisting FAs may also be transferred from membrane lipids into TAG via transacylation. Characterization of *C. reinhardtii*'s phospholipid:diacylglycerol acyltransferase (PDAT) revealed that it has both substantial lipase and acyltransferase activities, and is capable of removing FAs from a wide variety of glycerolipids and releasing them as free FAs or transferring them to diacylglycerol (DAG) to form TAG (Yoon et al., 2012). However, PDAT-deficient cells accumulate TAG at only slightly reduced rates, implying that other mechanisms contribute to TAG accumulation under N-deprivation.

While there have been many studies investigating the effects of N-deprivation on lipid production in algae, there have been relatively few analyzing the reprogramming that occurs when N is resupplied to the cells (Tsai et al., 2018), despite the importance of membrane resynthesis to the resumption of growth when stress conditions are relieved. Evidence has been found that FAs from TAG degradation can be used in membrane lipid synthesis, as radiolabeled 18:1 supplied during N-starvation and incorporated as 20:4 into TAG resulted in a decrease in radioactivity in TAG and an increase in chloroplastic lipids during N-resupply without a label (Khozin-Goldberg et al., 2005). Studies have also found that in the initial stage of N-resupply, the total FA content per cell is unchanged and there is no detectable de novo FA synthesis (Allen et al., 2017; Tsai et al., 2018), indicating that FAs from TAG may enter the membrane lipid pool during N-resupply. In addition, several *C. reinhardtii* TAG lipases (CrLIPs) that aid in the breakdown of TAG have been characterized (Li et al., 2012b; Warakanont et al., 2019), and the resulting free FAs may be recycled for membrane lipid synthesis during N-resupply. Loss-of-function mutants in a TAG lipase ortholog to Arabidopsis's Sugar-dependent 1 (CrLIP-4) were found to have reduced levels of polyunsaturated FAs (PUFAs) characteristic of membrane lipids compared to wild-type during N-resupply (Warakanont et al., 2019), implying that mutants impaired in TAG breakdown are also impaired in resynthesizing membrane lipids. Additionally, the *compromised hydrolysis of triacylglycerols 7* mutant is unable to degrade TAG following N-resupply and is also impaired in exiting the quiescent state of N-deprivation (Tsai et al., 2014). MGDG levels in this mutant recover less well than in wild-type cells following N-resupply (Tsai et al., 2018), further suggesting that TAG degradation and membrane lipid resynthesis are linked.

Several studies have reported evidence of membrane lipid recycling into TAG during N-deprivation based on measurements of FAs that are specific to particular lipids (Simionato et al., 2013; Allen et al., 2015). Thus, a decrease

in a particular FA in a membrane lipid class and a corresponding increase in that FA in TAG can indicate a transfer of that FA from membrane lipids into TAG. However, some major FAs in *C. reinhardtii* and other species are not diagnostic of de novo synthesis versus acyl chain recycling, some FAs are found in several different membrane lipids, and FA desaturation and elongation are highly active processes, making it difficult to pinpoint their sources. Direct measurements of the synthesis of FAs and their transfer into and between lipid pools require time course experiments using isotopically labeled substrates, as well as quantitation of levels and label composition of lipids and their FAs. Isotopic labeling was used in several studies to investigate the movement of FAs between polar lipids and TAG (Khozin-Goldberg et al., 2005, Goncalves et al. 2013; Juergens et al., 2016; Allen et al., 2017; Pick and Avidan, 2017). ^{14}C pulse-chase labeling revealed reciprocal changes in the levels of radioactivity in membrane lipids and TAG during N-deprivation in *Chlorella protothecoides* (Gonclaves et al. 2013) and N-resupply in *Parietochloris incisa* (Khozin-Goldberg *et al.* 2005). In *Dunaliella tertiolecta*, $^{14}CO_2$ labeling showed that starch synthesized before or early during N-deprivation is turned over during N-deprivation and label accumulated concomitantly in TAG, indicating a substantial contribution to TAG synthesis of carbon from starch (Pick and Avidan, 2017). ^{13}C pulse-chase labeling during N-deprivation of *C. reinhardtii* and measurement of label distributions in starch, TAG, and several FAs in different membrane lipid classes revealed high rates of simultaneous synthesis and degradation of major membrane lipids and a high contribution (~75%) of carbon assimilated during the course of N-deprivation to TAG synthesis, but little contribution from starch (Juergens et al. 2016). An analysis of the time course of ^{13}C and ^{2}H isotopic distribution in lipids of the polar microalga *Coccomyxa subellipsoidea* after labeling prior to N-deprivation with different substrates also showed membrane lipid turnover involving glyceryl backbones as well as FAs, and that a high proportion of FAs incorporated into TAG during N-deprivation were derived from carbon assimilated during N-deprivation, with ~20% of FAs incorporated into TAG throughout N-deprivation being from preexisting FAs in membrane lipids (Allen et al., 2017). The results of a recent study of *Nanochloropsis gaditana* using $^{13}CO_2$ labeling prior to N-deprivation provided evidence for the movement of C20:5 from membranes to TAG during N-starvation, with this transfer accounting for approximately one-third of C20:5, and ~2% of total FA accumulation in TAG in the first phase of N-deprivation and little of the subsequent accumulation (Janssen et al., 2019). In that study, FA synthesis from external and nonlipid internal carbon sources accounted for the vast majority of TAG synthesis.

It is therefore clear that preexisting polar lipids contribute to TAG synthesis, but questions remain about (1) their quantitative contribution to TAG synthesis, (2) which polar lipid FAs make substantial contributions to which FAs accumulating in TAG, (3) the extent to which membrane lipid FAs made before TAG accumulation are conserved during TAG synthesis, as they turn over and often decrease during nutrient deprivation, (4) the fate of total and individual FAs during TAG breakdown after nutrient limitation is relieved, and related to this (5) the contribution of preexisting FAs and other biomass components to the synthesis of membrane lipids as growth resumes upon nutrient resupply. To address these questions and begin to reveal precursor–product relationships, as well as quantify fluxes of newly synthesized and preexisting lipid components during TAG synthesis and degradation, measurement of concentrations as well as absolute levels and intramolecular patterns of labeling is required, preferably in a model organism under well-studied conditions. In addition, analysis of labeling in major non-lipid cell components is required to assess the potential contribution of preexisting biomass to label distribution.

In this study, we determined the relative contribution of de novo synthesis and membrane lipid recycling to the accumulation of FAs in TAG during N-deprivation, and the contribution of TAG acyl chains to membrane lipid synthesis during N-resupply and growth. Time course experiments involving successive periods of N-replete growth, N-deprivation, and N-resupply were performed in which [1-^{14}C]acetate (for sensitive analysis of total label in different lipid classes) and [$^{13}C_2$]acetate (for quantifying fractional labeling and distribution of label across different FAs in each lipid class) were provided either before or during the N-deprivation phases (Figure 1). The results show that during N-deprivation, much of the PUFAs incorporated into TAG (particularly 16:4 and 18:3Δ9,12,15, hereafter referred to as 18:3α) come from membrane lipids made prior to N-deprivation, while most of the saturated, mono-, and di-

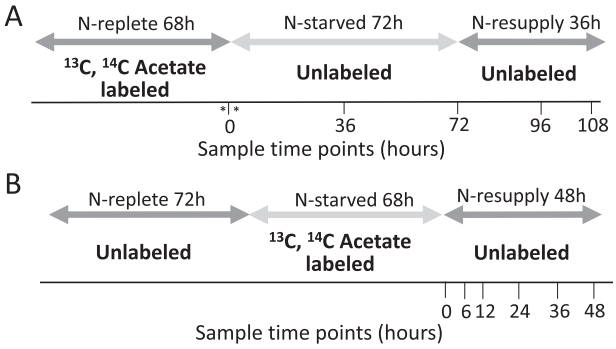

Figure 1 Experimental design of labeling schemes. A, Illustration in which [1-^{14}C]- and [$^{13}C_2$]-acetate were applied during N-replete growth, followed by an unlabeled N-deprived period of 72 h. An unlabeled N-resupply period of 36 h followed. Asterisks around time 0 indicate samples taken before and just after transfer to N-deprived medium shown in Supplemental Figure S9. B, Illustration in which [1-^{14}C]- and [$^{13}C_2$]-acetate were applied during a 68 h N-deprivation period, followed by an unlabeled N-resupply period of 48 h. Samples were collected at each time point indicated. Dark gray arrows indicate N-replete conditions, while light gray arrows indicate N-deprived conditions.

unsaturated FA moieties in TAG are made de novo from exogenous carbon during deprivation. During the initial stage of N-resupply, the majority of FAs used in membrane lipid synthesis are derived from TAG degradation. Remarkably, despite large FA fluxes from membrane lipids into TAG synthesis during N-deprivation and back from TAG into new membrane lipids during recovery and growth following N-resupply, there is no significant loss of the FA carbon originally assimilated into FAs during N-replete growth. These results show that TAG has a major role as a storage pool for acyl chains from membrane lipids in order to facilitate the rebuilding of membrane lipids upon resupply of N for rapid recovery and resumption of growth.

Results

Overview of labeling schemes

Two different labeling schemes were applied in this study, both utilizing [1-^{14}C]- and [$^{13}C_2$]-acetate as the labeling substrates, in order to follow the fate of FAs synthesized before or during N-starvation. When acetate is supplied in the medium it is taken up by the cells, converted to acetyl-CoA, and utilized as the building block for FA biosynthesis. Thus, using labeled acetate allows one to track the incorporation of newly synthesized and previously synthesized FAs into different lipids. In one scheme, [1-^{14}C]- and [$^{13}C_2$]-acetate were employed prior to N-deprivation (timecourse A) in order to quantify the acyl chain transfer from membrane lipids into TAG (Figure 1A). In the other scheme, [1-^{14}C]- and [$^{13}C_2$]-acetate were supplied during N-deprivation (timecourse B) in order to trace the flux of FAs from TAG into membrane lipids during N-resupply (Figure 1B).

Cell growth and lipid content during N-starvation and resupply

As indicators of cell response to N-deprivation and resupply, cellular growth, biomass (as reflected by optical density [OD] measured at 750 nm [OD_{750}]), chlorophyll levels, and the levels and FA contents of major lipid classes were measured. Cell growth and division halted during N-deprivation (Figure 2A). While some studies have found that cells undergo one additional doubling during N-deprivation (Lee et al., 2012; Msanne et al., 2012), another using cell wall-less strains also found a nearly immediate halt in cell division during N-deprivation (Work et al., 2010). Chlorophyll levels per cell fell during N-deprivation, and visible signs of chlorosis were also observed during N-deprivation, while regreening occurred within 12 h following N-resupply (Figure 2B). The OD_{750} increased during N-deprivation due to the accumulation of starch and lipid rather than cell growth and division (Figure 2C). As previously reported in Tsai et al. (2018), cell growth and division resume after N-resupply following a 12-h lag period (Figure 2, A and C) during which chlorophyll is synthesized, and growth has recovered by ~24 h of N-resupply (Figure 2B). The quantity of TAG per culture volume and per cell increased during N-deprivation, while the levels of membrane lipids per culture volume did not change significantly (Figure 3A; Supplemental Figure S1). Previous studies have reported that during N-deprivation, membrane lipid levels per cell decrease (Siaut et al., 2011) or remain unchanged (Fan et al., 2011). MGDG decreased during N-deprivation as a proportion of total polar lipids while digalactosyldiacylglycerol (DGDG; Fan et al., 2011; Li et al., 2012a) and diacylglyceryltrimethylhomoserine (DGTS) increased (Yang et al., 2020), and the proportion of sulfoquinovosyldiacylglycerol (SQDG) and phosphatidylethanolamine (PE) did not change significantly (Figure 3B). We did not quantify the levels of phosphatidylglycerol and phosphatidylinositol, which each constitute only 5%–7% of glycerolipids in *C. reinhardtii* (Li-Beisson et al., 2015). Following N-resupply, the proportion of MGDG returned to its pre-deprivation level and the proportions of DGDG and DGTS fell back to levels close to those before N-deprivation (Figure 3B). FAs from total cellular lipid extracts showed that the proportion of total FA accounted for by those that are abundant in TAG (18:1Δ9 and 18:2) versus membranes (18:3α and 16:4) rose and fell in concert with the relative levels of TAG and membrane lipids (Figure 3C).

Quantity and labeled acetate incorporation in total cellular fatty acids

Cellular levels of FAs rose during N-deprivation (Figure 4A; Shifrin and Chisholm, 1981; Livne and Sukenik, 1992; Moellering and Benning 2010), demonstrating the net synthesis of FAs. The level of total cellular FAs per culture volume was not significantly changed during the first 24 h of N-resupply, after which it rose (Figure 4, A and B; Allen et al., 2017; Tsai et al., 2018). When cells were labeled with [1-^{14}C]- and [$^{13}C_2$]-acetate either before or during N-deprivation, the amount of ^{14}C label in FAs from total cellular lipid extracts did not change significantly through subsequent N-deprivation and resupply periods (Figure 4, A and B). In addition, when cells were labeled prior to N-deprivation, the level of highly ^{13}C-labeled FAs from total cellular lipid extracts did not change significantly through subsequent unlabeled N-deprivation and resupply periods (Figure 4, C–F). These observations suggest that the carbon of FAs made either before or during N-deprivation remains in the total FA pool throughout N-deprivation and resupply.

Labeling from ^{14}C-acetate indicates acyl exchange between TAG and membrane lipids

When cells were labeled with [1-^{14}C]- and [$^{13}C_2$]-acetate during exponential growth in N-replete medium and transferred to unlabeled medium during N-deprivation and subsequent N-resupply (Figure 1A), the rise in TAG quantity per culture volume during N-deprivation and its fall during N-resupply were closely tracked by the levels of radioactivity in TAG (Figure 5A). Thus, TAG synthesis includes a substantial contribution from preexisting cellular contents, which are then lost from TAG during recovery from N-deprivation. In contrast, membrane lipid levels per culture volume stayed

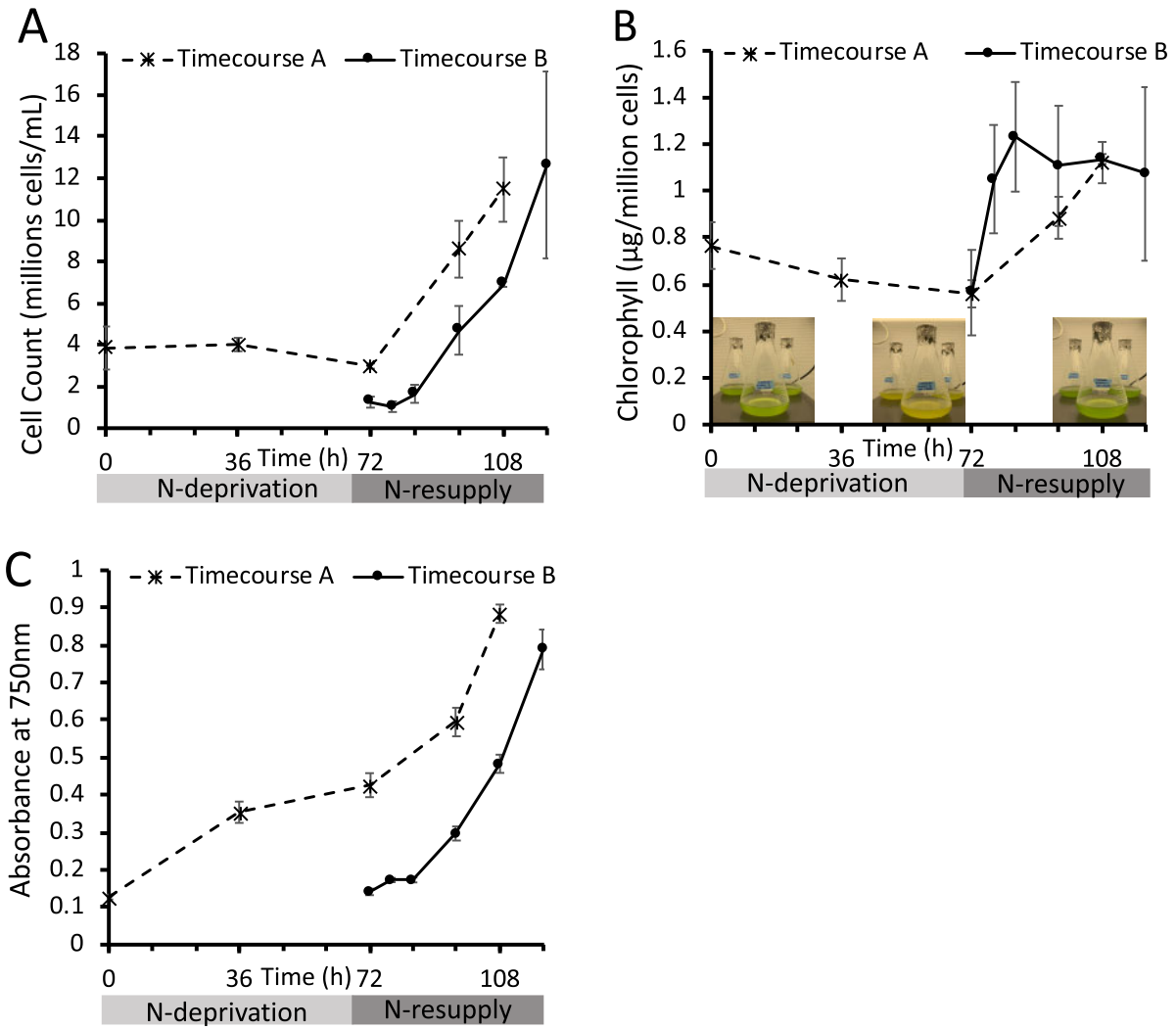

Figure 2 Cell growth and chlorophyll levels recover upon N-resupply. A, Cells counted using a hemocytometer. B, Chlorophyll extracted in 3:2 Acetone:DMSO and quantified spectroscopically. Images of cultures at different stages of N-deprivation and resupply are overlaid. C, OD measured at 750 nm using a DU 800 spectrophotometer (Beckman Coulter). "Timecourse A" and "Timecourse B" refer to the two experimental timecourses outlined in Figure 1, which used different labeling schemes and initial cell densities. Error bars indicate ±SD (n = 3).

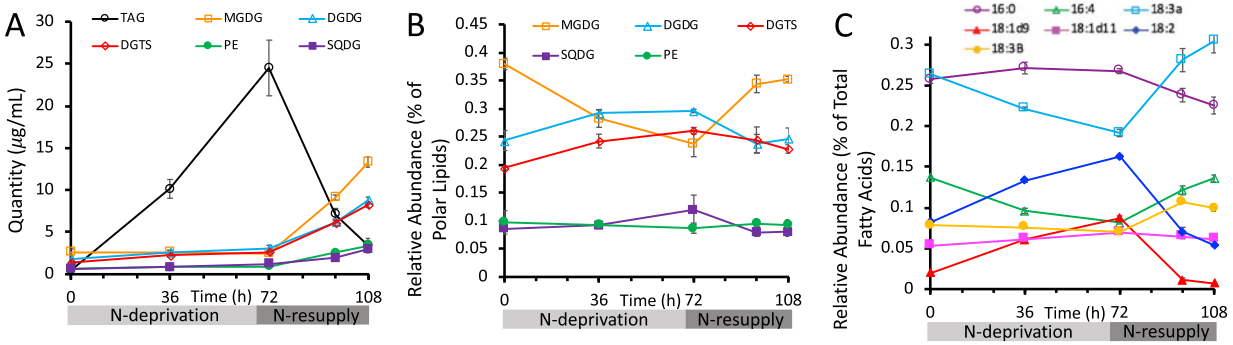

Figure 3 Lipid classes and total FAs during N-deprivation and resupply. A, Quantity of major lipid classes, quantified by summation of all FAMEs detected using an Agilent GC-FID with a DB-23 column and normalization to an internal standard. B, Relative abundance of major polar lipid classes. C, Relative abundance of total cellular FAs, quantified by Gas Chromatography-Flame Ionization Detection of transmethylated total lipid extracts. All panels represent data from timecourse A, error bars indicate ±SD (n = 3).

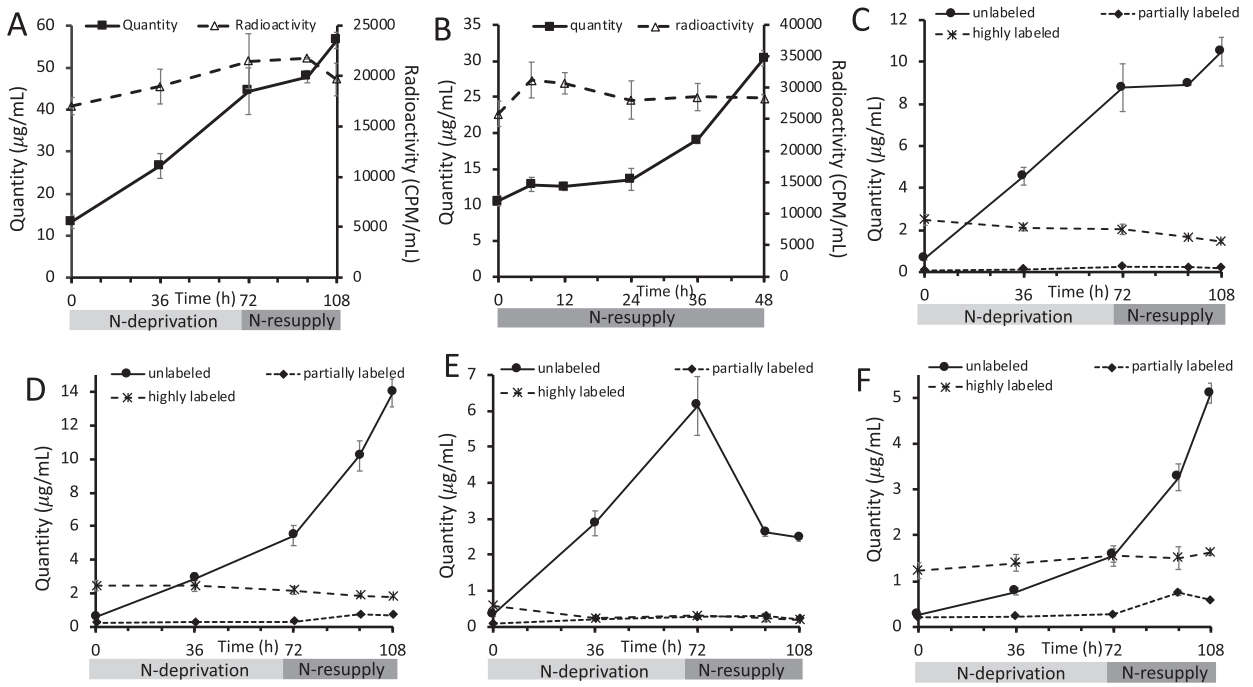

Figure 4 Levels and ^{14}C- and ^{13}C-acetate incorporation in total cellular FAs. Levels and radioactivity of total FAs in the cells during experiment in which labeled acetate was applied prior to N-deprivation (A) or during the experiment in which labeled acetate was applied during N-deprivation (B). In (A), ^{14}C in total FAs did not change significantly during the N-deprivation and resupply period according to a two sample *t* test assuming unequal variances implemented in Microsoft Excel between the first and last timepoint ($P = 0.09$). Quantity of total cellular FAs divided into low, intermediate, and high levels of ^{13}C-acetate incorporation for 16:0 (C), 18:3α (D), 18:2 (E), and 16:4 (F) in timecourse A. Here and elsewhere, we refer to FAs as "highly labeled" if at least two-third of the molecule is ^{13}C-labeled, we use "unlabeled" to refer to molecules with no ^{13}C-label (M_0), and "partially labeled" indicates molecules that are greater than M_0 but contain less than two-third ^{13}C-label. Error bars indicate ±SD ($n = 3$).

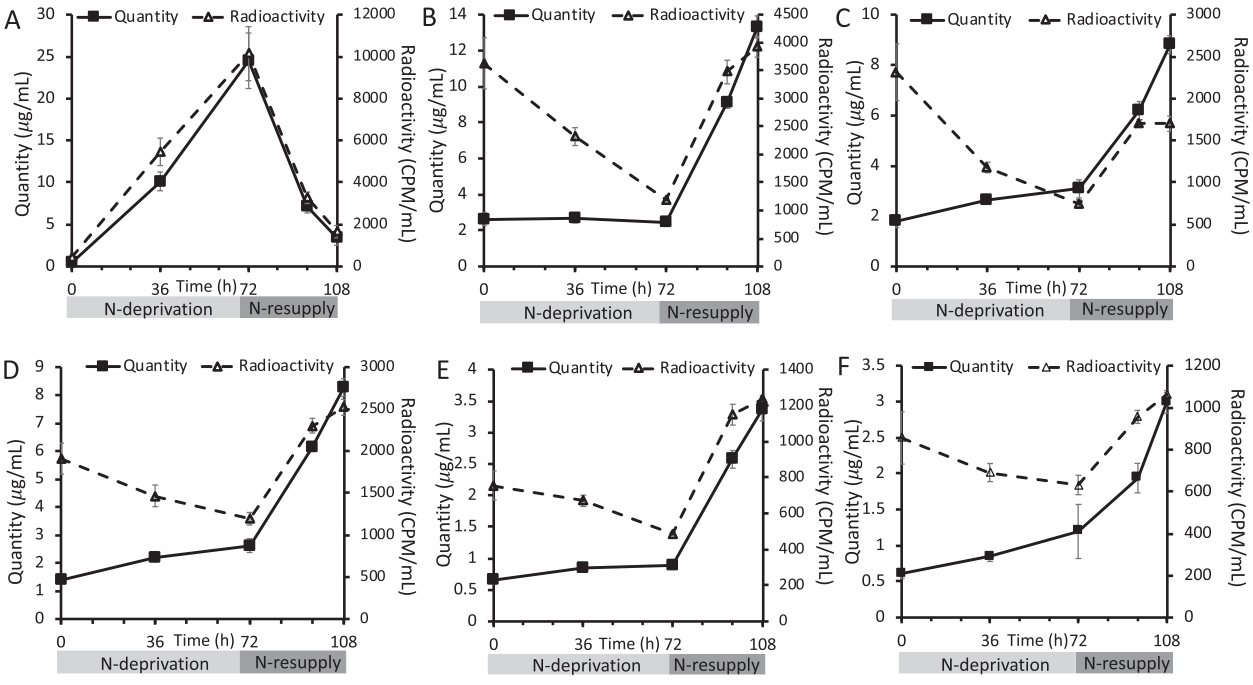

Figure 5 Quantity and level of radioactivity in different lipid classes during N-deprivation and resupply in timecourse A. Quantity and radioactivity of TAG (A), MGDG (B), DGDG (C), DGTS (D), PE (E), and SQDG (F) during experiment in which labeled acetate was applied prior to N-deprivation (Figure 1A). Lipid extracts were separated on TLC plates, individual bands were scraped off, converted to FAMEs, and quantified via GC-FID. Radioactivity in the resulting FAMEs was measured via liquid scintillation counting. Error bars indicate ±SD ($n = 3$).

constant or rose slightly during N-deprivation, while radioactivity levels in those lipids fell (Figure 5, B–F), demonstrating that turnover of membrane lipids during N-deprivation was substantial and involves removal of preexisting FAs and their replacement by FAs synthesized from newly assimilated carbon. Previous labeling experiments have also found evidence of membrane lipid turnover during N-deprivation (Juergens et al., 2016; Allen et al., 2017). The level of radioactivity in TAG is inversely correlated with that in membrane lipids, suggesting the exchange of ^{14}C-labeled FAs between the two pools (Figure 5). The reciprocal changes in total radioactivity in membrane lipids versus TAG appear unequal because less abundant lipids are less efficiently recovered from thin-layer chromatography (TLC) plates and because lower abundance lipids were not assayed for radioactivity. Direct analysis of total lipid FA methyl esters (FAMEs) avoids these distortions and shows that the radioactivity in FAs from total lipid extracts did not change significantly throughout the time-course, thus supporting the idea that losses of radioactivity in membranes during N-deprivation are equivalent to the gain in radioactivity in TAG, and vice versa during N-resupply (Figure 4A). In addition, the amount of radioactivity in the chloroplastic lipid DGDG returns to a lower level than that before N-deprivation following N-resupply, while the labeling in extraplastidial lipids DGTS and PE exceed their beginning levels (Figure 5, C–E). This suggests that acyl chains supplied from TAG that aid in membrane lipid resynthesis following N-resupply favor extraplastidial lipid assembly over chloroplastic lipid synthesis.

When cells were labeled with [1-^{14}C]- and [$^{13}C_2$]-acetate during N-deprivation (Figure 1B), the amount of radioactivity in TAG fell in parallel with the decreasing TAG levels during N-resupply in unlabeled medium (Figure 6A). Concomitantly, radioactivity in membrane lipids rose as their levels per culture volume increased (Figure 6, B–F). The amounts of radioactivity in the different membrane lipids reached plateaus after 24–36 h as the amount of TAG fell to low levels (Figure 6), supporting the idea that TAG is the source of radiolabel for membrane lipids. The decrease in radiolabel in TAG accounts quantitatively for the sum of the increases in radiolabel measured in the major membrane lipid classes, which indicates that the carbon lost from TAG during N-resupply is used in the synthesis of membrane lipids. There are a number of possible routes by which the radiolabeled carbon in TAG could reach membrane lipids, and the ^{13}C labeling analyses detailed below help discern among transfer of intact FA molecules versus indirect routes such as β-oxidation and resynthesis.

Membrane lipid PUFAs contribute to TAG synthesis during N-deprivation and TAG returns acyl chains for membrane lipid resynthesis during N-resupply

The use of ^{13}C acetate as a labeling substrate allows the distribution of mass isotopomers in different FAs to be determined by Gas Chromatography–Mass Spectrometry . Unlabeled FA molecules not made during labeling can be quantified separately from highly labeled ones produced directly from fully labeled substrates. Partially labeled molecules produced from partially labeled substrates, or from a combination of highly labeled and less labeled ones, can also be distinguished. Our coverage of levels and labeling of FAs in individual lipid classes was at least 95%, with the exception of the less abundant lipid PE for which our coverage of its FAs was 89%. When cultures were labeled during exponential growth and then transferred to unlabeled, N-deprived tris–acetate–phosphate (TAP) medium (Figure 1A), PUFAs, particularly 18:3α and 16:4, that accumulated in TAG during N-deprivation included high proportions of highly labeled molecules (Figure 7A), indicating that these FAs came from preexisting membrane lipids made prior to N-deprivation. Levels of most highly labeled FA species in membrane lipids fell during N-deprivation and rose during N-resupply (Figure 7, B–D), suggesting extensive FA exchange with TAG. Levels of saturated and mono- or di-unsaturated FAs in TAG also rose strongly during N-deprivation, but accumulated very little labeled carbon (Figure 7A), showing that these were synthesized de novo during N-deprivation from exogenous carbon acquired during the unlabeled deprivation period. Consistent with this inference, when ^{14}C- and ^{13}C-acetate label were supplied during N-deprivation (Figure 1B), most of the FA species accumulating in TAG were highly labeled, but PUFAs such as 16:4, 18:3α, and 18:3Δ5,9,12 (18:3β) contained nearly equivalent amounts of unlabeled and highly labeled FAs (Figure 8; Supplemental Figure S2), further indicating that a high portion of these PUFAs in TAG came from preexisting membrane lipids made during N-replete growth.

In addition to the increases in highly labeled FAs (Figure 7, B–D), some membrane lipid FA pools showed increasing levels of partially labeled FAs during the N-resupply period. Partially labeled FA molecules can arise from several sources, such as breakdown and resynthesis of FAs by β-oxidation (Eccleston and Ohlrogge, 1998) or utilization of partially labeled starch and proteins for FA synthesis. However, perhaps surprisingly in light of past reports (Pick and Avidan, 2017; Janssen et al., 2019) and the large rates of membrane lipid turnover and of TAG accumulation and breakdown, these partially labeled FA molecules constitute only a small proportion of FA molecules at any time. Of the FAs accumulated in membrane lipids in the first 24 h of N-resupply, only 6% of the total FAs in membrane lipids were partially labeled (Figure 7, B–D; Supplemental Figures S3 and S4). The degree of partial labeling varied among individual FAs, with some such SQDG 16:0 as low as 1.6% (Supplemental Figure S3) and DGTS 16:4 as high as 21% (Supplemental Figure S4), indicating different turnover rates among some FA pools. Overall, breakdown of highly labeled FAs via β-oxidation followed by resynthesis appears to be at most a modest route of FA flux into membrane lipids during N-resupply.

When ^{14}C- and ^{13}C-acetate label was supplied during N-deprivation and cultures were transferred to unlabeled N-resupply medium (Figure 1B), the amounts of highly ^{13}C-

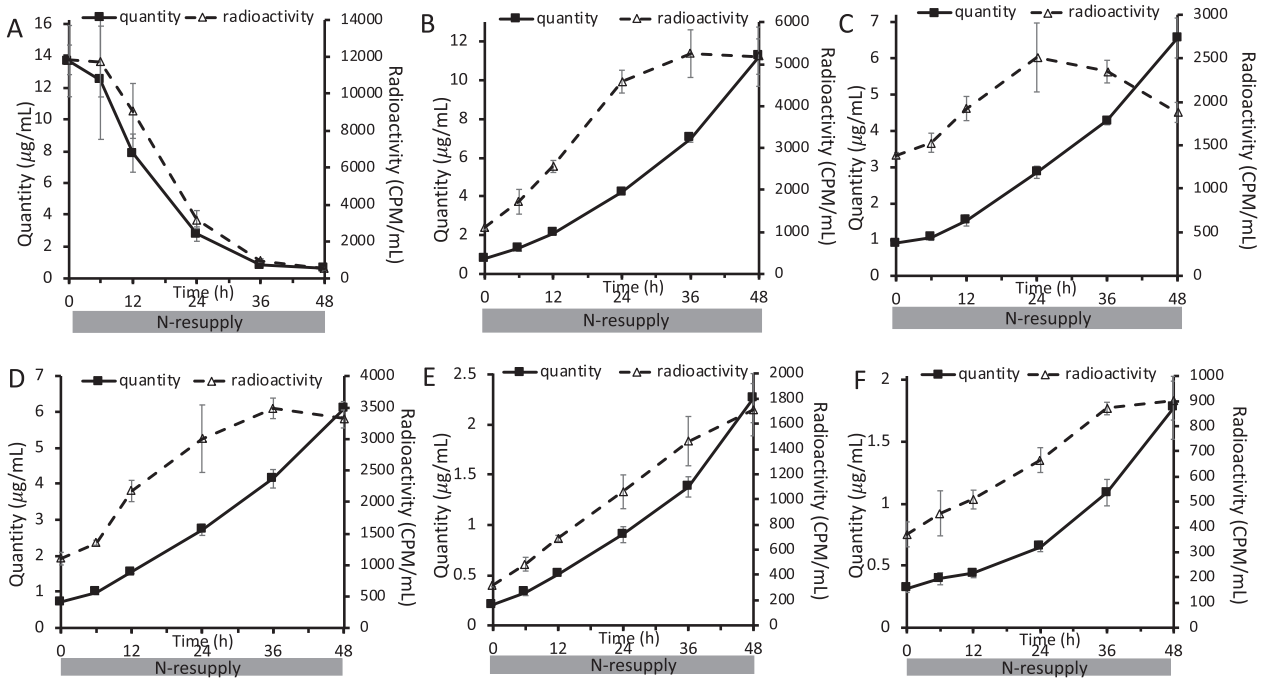

Figure 6 Quantity and level of radioactivity of different lipid classes during N-resupply in timecourse B. Quantity and radioactivity of TAG (A), MGDG (B), DGDG (C), DGTS (D), PE (E), and SQDG (F) during the experiment in which labeled acetate was applied during N-deprivation followed by an unlabeled N-resupply period (Figure 1B). Lipid extracts were separated on TLC plates, individual bands were scraped off, converted to FAMEs, and quantified via GC-FID. Radioactivity in resulting FAMEs was measured via liquid scintillation counting. Error bars indicate ±SD (n = 3).

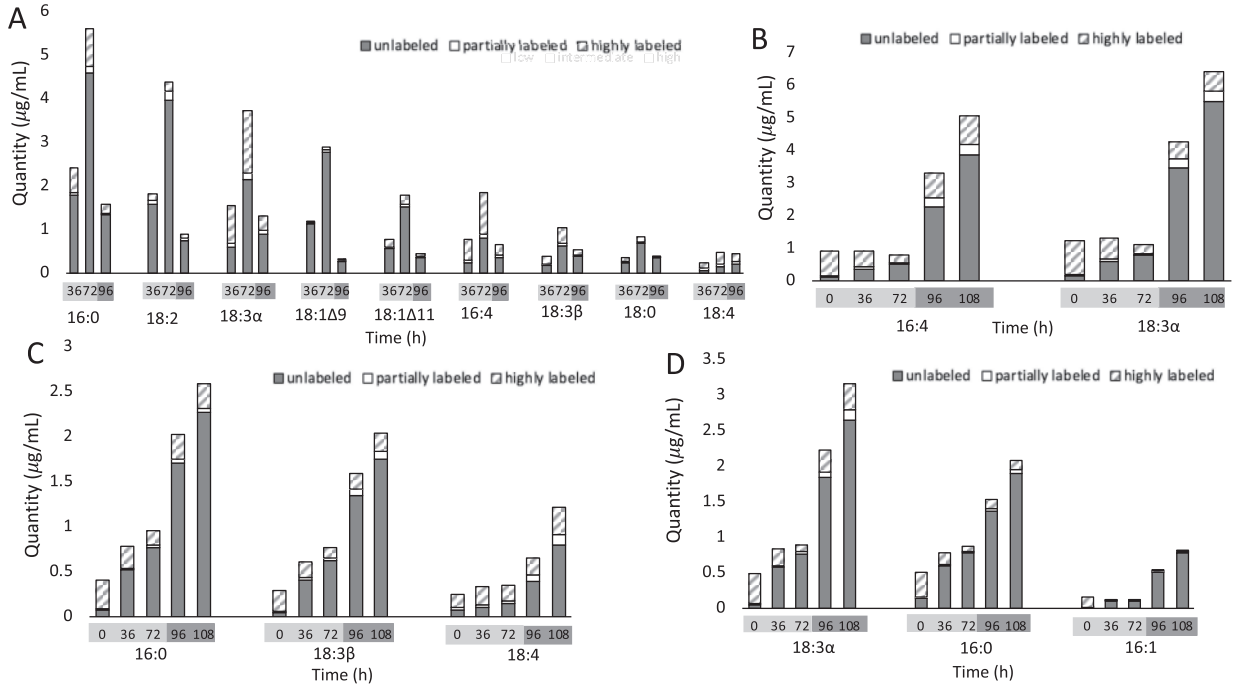

Figure 7 ^{13}C-labeled and unlabeled FA content of major lipid classes in timecourse A. Quantity of FAs divided into low, intermediate, and high levels of ^{13}C-acetate incorporation are shown for TAG (A), MGDG (B), DGTS (C), and DGDG (D) FAs during N-deprivation and resupply. Bars represent an average of three biological replicate cultures in experimental timecourse A (see Materials and Methods section). Error is not shown, although data ±SD in line graph form is shown in Supplemental Figures S3, S4, and S8.

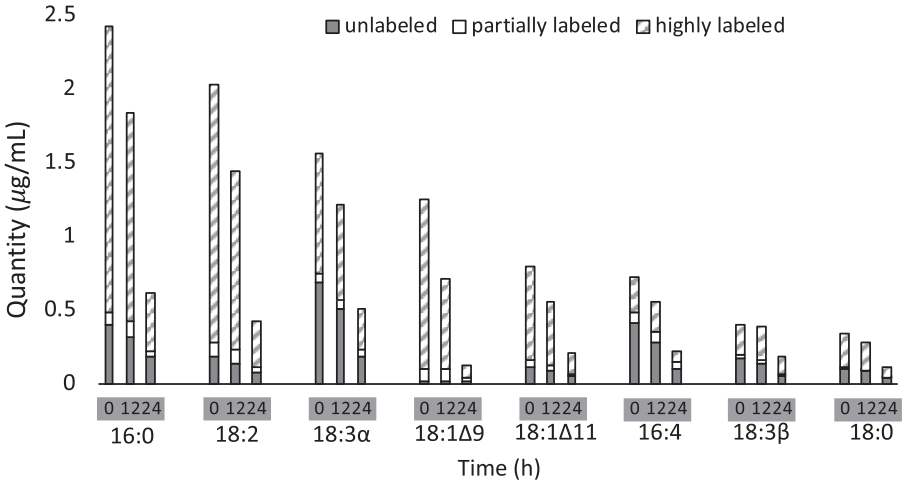

Figure 8 ^{13}C-labeled and unlabeled FA content of TAG during N-resupply in timecourse B. Quantity of TAG FAs divided into low, intermediate, and high levels of ^{13}C-acetate incorporation. Bars represent an average of three biological replicate cultures in experimental timecourse B (see Materials and Methods section). Error is not shown, although data ±SD in line graph form is shown in Supplemental Figure S2.

labeled FAs in membrane lipids rose during N-resupply, and the majority of new membrane lipid synthesis in the first 24 h of N-resupply came from highly labeled acyl chains derived apparently from TAG (Figure 9). The incorporation of highly labeled FAs into membrane lipids plateaued as the amount of TAG approached zero (Figure 9), further indicating that they came from TAG. Once TAG was depleted during N-resupply, levels of unlabeled FA molecules in membrane lipids increased as de novo FA synthesis increased and became the source of the majority of new membrane lipid synthesis.

Starch and proteins do not contribute significantly to lipid synthesis during N-resupply

Starch accumulates to high levels during N-deprivation (Supplemental Figure S5), its levels rising linearly earlier and higher than TAG. Starch is also degraded more rapidly than TAG following N-resupply (Siaut et al., 2011; Juergens et al., 2016). Furthermore, ^{14}C labeling evidence points to starch synthesized before or early during N-deprivation as a source of carbon for subsequent TAG synthesis in *Dunaliella tertiolecta* (Pick and Avidan, 2017). Therefore, it is important to determine whether starch, and indeed other major biomass constituents, could be the source of precursors for lipid synthesis during N-resupply rather than lipids synthesized during N-deprivation. Starch from cells collected at the end of the N-deprived labeling period (Figure 1B) were hydrolyzed to glucose, derivatized, and their labeling patterns analyzed by GC–MS. Approximately 73% of the carbon in starch was found to be ^{13}C-labeled, but only approximately one-third of the glucose units were fully labeled (Figure 10A). This degree of labeling is consistent with most of the starch being synthesized during the labeling period, and the small proportion of unlabeled starch suggests that the preexisting starch was likely not turned over during the N-deprivation period (Figure 10A). From this label distribution, we simulated the expected label distribution in 16-carbon FA molecules if they were derived from carbon with the level of labeling observed in the starch pool. This distribution is compared to the measured mass isomer distribution of a DGDG 16-carbon FA sampled at 24 h after N-resupply in timecourse B (Figure 10B). These two distributions are very distinct. For example, the most abundant mass isomer expected if the FA were synthesized from starch carbon contains 12 ^{13}C and 4 ^{12}C atoms (Figure 10B). However, experimentally we observe that the highest proportions of molecules are either unlabeled or fully labeled (Figure 10B), which are predicted to very rare in FA made from the carbon of starch, and indicate that the biosynthetic precursors of the highly labeled FAs were $>90\%$ ^{13}C labeled. Thus, if starch were contributing substantial amounts of carbon to FA synthesis via breakdown to acetyl-CoA, a high proportion of FA molecules would be expected to be partially labeled, particularly in the range M + 8 – M + 13. The low levels of partially labeled FA molecules indicate that there is little contribution of starch to FA lipid synthesis during N-resupply. In addition, by 12 h of N-resupply the majority of the starch accumulated during N-deprivation has been depleted (Supplemental Figure S5), but the highly labeled acyl chains in membrane lipids continue to increase linearly from 12 to 24 h of N-resupply (Figure 9). Thus, we conclude that preexisting starch makes little or no contribution to FA synthesis during recovery from N-deprivation.

Proteins related to photosynthesis and the Calvin–Benson cycle have been found to decrease during N-deprivation, while those related to respiratory complexes increase (Schmollinger et al., 2014). This aligns with the notion that photosynthesis is downregulated during N-deprivation, and the cells display a preference for respiration. Protein synthesis decreases during N-deprivation and recovers rapidly upon N-resupply (Tsai et al., 2014), therefore proteins were digested to amino acid units, derivatized, and analyzed by GC–MS at the end of the labeled N-deprivation period (Figure 1B) to determine the potential contribution of this

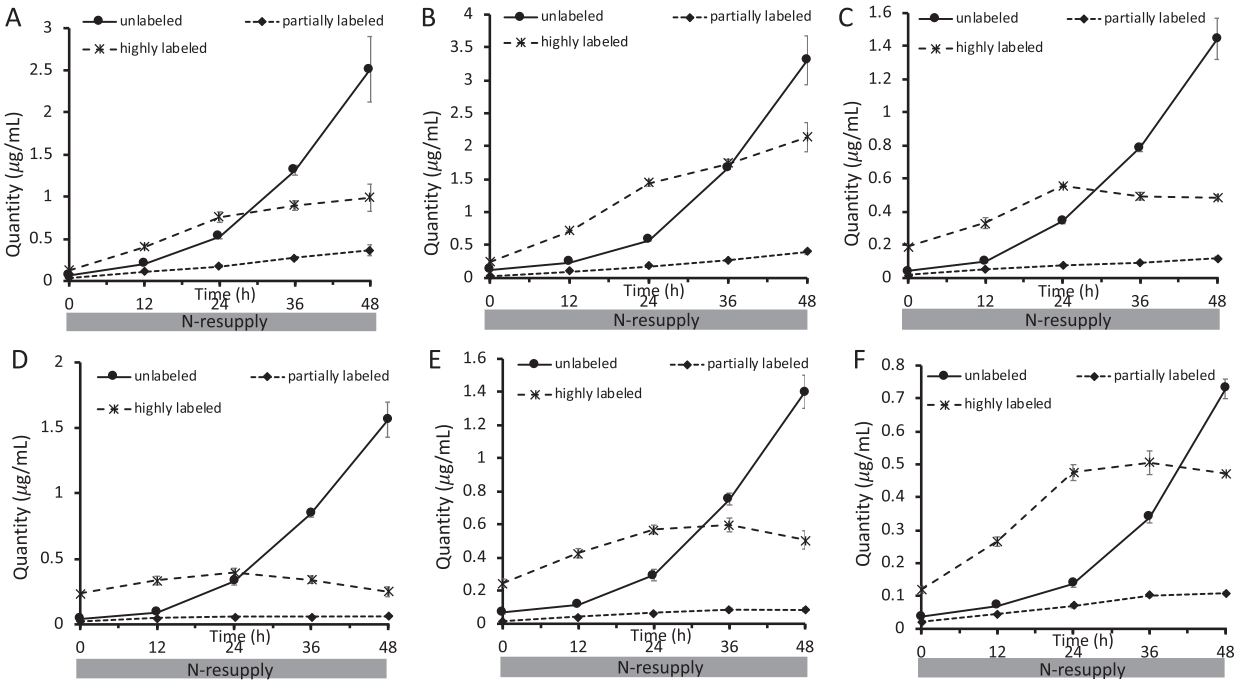

Figure 9 ^{13}C-acetate incorporation in FAs in polar lipid classes during N-resupply in timecourse B. Quantity of FAs divided into low, intermediate, and high levels of ^{13}C-acetate incorporation are shown for MGDG 16:4 (A), MGDG 18:3α (B), DGDG 18:3α (C), DGDG 16:0 (D), DGTS 16:0 (E), and DGTS 18:3β (F). Error bars indicate ±SD (n = 3).

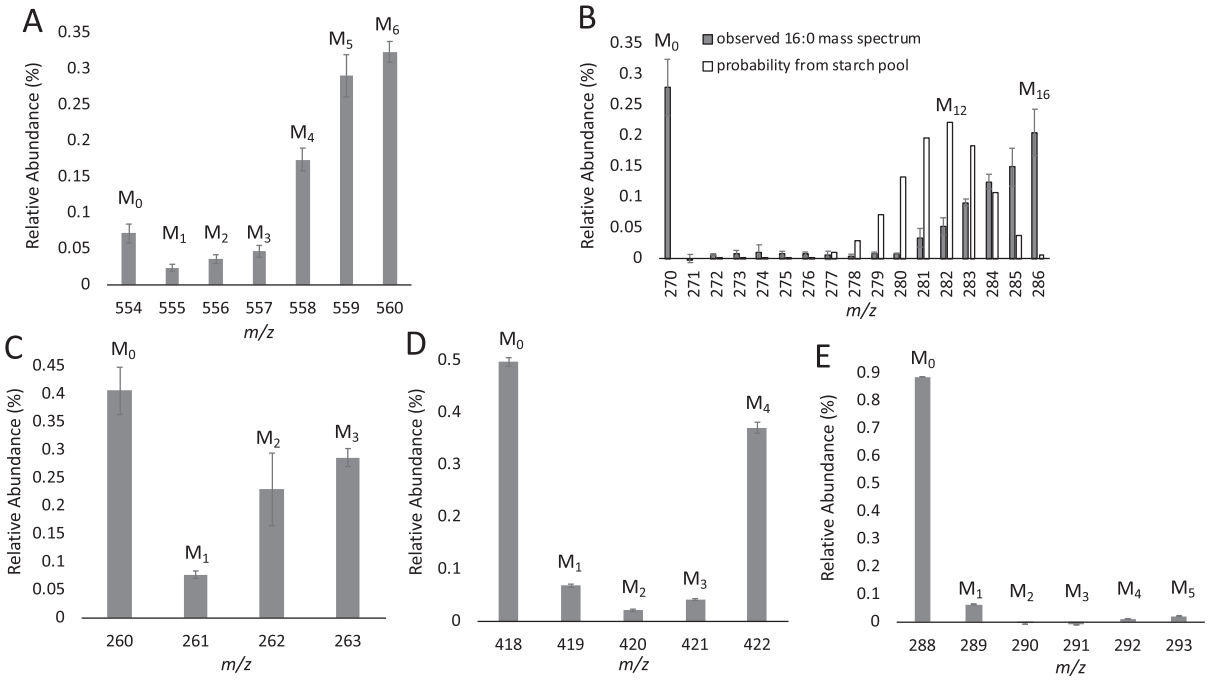

Figure 10 ^{13}C isotopomer distribution of glucose units from hydrolyzed starch and amino acids from hydrolyzed protein at the end of the N-deprivation labeling period in timecourse B. Mass isomer distributions are shown for glucose from hydrolyzed starch (A) and a 16:0 FA from DGDG at 24 h of N-resupply with a binomial distribution overlaid showing the probability of deriving an 16-carbon FA with varying degrees of labeling from the starch pool (B). Mass isomer distributions are shown for amino acids alanine (C), aspartate (D), and valine (E). Error bars indicate ±SD (n = 3) for glucose (A) and FA (B), and error bars indicate range (n = 2) for amino acids (C–E).

pool to new lipid synthesis during N-resupply. The amino acid alanine is synthesized from pyruvate, and ~47% of the carbon in alanine is ^{13}C-labeled (Figure 10C). Amino acids synthesized from tricarboxylic acid cycle (TCA) cycle intermediates, such as aspartate, contain about half unlabeled molecules and about half fully labeled molecules (Figure 10D; Supplemental Figure S6), and from this, we can deduce that TCA cycle intermediates are labeled during N-deprivation, as would be expected given the evidence for substantial induction of respiration enzymes during N-deprivation (Schmollinger et al., 2014). Certain amino acids with low turnover rates consist almost entirely of unlabeled molecules (Figure 10E; Supplemental Figure S6). Thus, despite the lack of protein synthesis during N-deprivation, the observed increase in ^{13}C-label in certain amino acids (Figure 10, C–E; Supplemental Figure S6) demonstrates that turnover of proteins occurs even in the absence of N. Although the amino acid pool contains a mixture of unlabeled and highly labeled molecules, overall the degree of isotopic labeling in the amino acid pool is much below that required to serve as carbon precursors for the highly labeled FA molecules observed during N-resupply. Representative spectra of membrane lipid FAMEs during N-resupply in timecourse B are shown in Supplemental Figure S7 to demonstrate the degree of labeling in this fraction. The distribution of ^{13}C-label in membrane lipid FAMEs much more closely resembles that of TAG FAMEs at the end of the N-deprivation labeling period than it does that of starch or proteins (Supplemental Figure S7). Based on the isotopic labeling profiles of glucose from starch and amino acids from proteins, the synthesis of membrane lipids during N-resupply containing highly labeled FA molecules is not from the bulk starch or protein pools.

Discussion

TAG is assembled from both preexisting and newly synthesized FAs

Our results show that in addition to FAs from de novo synthesis, TAG also accumulates preexisting FAs from membrane lipids during N-deprivation (Figures 7, A and 8). FA molecules newly synthesized during N-deprivation may be exported from the plastid and directly incorporated into TAG, or first be incorporated into membrane lipids prior to transfer into TAG. Previous work has identified a route by which 18:1Δ9 is incorporated into MGDG and subsequently into TAG via the lipase PGD1 (Li et al. 2012a), and other authors have concluded from radiolabeling (Pick and Avidan, 2017) and lipid profiling (Yang et al., 2020) that some fraction of the FA molecules made during N-deprivation that accumulate in TAG were first incorporated into membrane lipids. Our results show that membrane lipids are simultaneously synthesized and broken down during N-deprivation (Figure 5, B–F), with ~84% of preexisting FA species in the major lipid classes being largely or entirely replaced within 3 d of N-deprivation, with interesting exceptions such as SQDG 16:0 and DGTS 18:4 (Supplemental Figures S3 and S4). It, therefore, seems likely that some of the FAs newly synthesized and incorporated into membrane lipids during N-deprivation subsequently flow into TAG. In both of the labeling schemes analyzed, we observed that a portion of the PUFAs in TAG must have been synthesized during the N-deprivation period (Figures 7, A and 8). It is known that in *C. reinhardtii*, membrane lipids act as substrates for desaturation of FAs (Giroud and Eichenberger, 1989), such as the Δ4 desaturase that acts specifically on MGDG to synthesize 16:4 (Zäuner et al., 2012). This, and the absence of known desaturases acting on TAG makes it reasonable to assume that PUFAs made during N-deprivation and accumulated in TAG were first incorporated into membrane lipids as saturated or mono-unsaturated FAs and were desaturated there prior to being incorporated into TAG. Thus, membrane lipids serve as both suppliers of preexisting FAs to TAG and as intermediate pools into which newly synthesized FAs are incorporated and either desaturated (PUFAs) or not (as in the case of PGD1) en route to accumulating in TAG.

Three different routes of acyl chain flux into TAG

Previously, it has been concluded that the large majority of TAG is made de novo during N-deprivation in *C. reinhardtii* and other algae. Evidence for flux of 18:1 through MGDG via PDG1 during N-deprivation indicates that some of the newly made FA is transiently incorporated in membrane lipids prior to its accumulation in TAG (Li et al., 2012a). Here, we demonstrate that a route of acyl chain flux into TAG coming from preexisting membrane lipids makes a large contribution to TAG synthesis. Three routes of FA flux into TAG during N-deprivation are illustrated schematically in Figure 11. In the first route, preexisting membrane lipids are turned over, releasing FAs made before N-deprivation, which are then incorporated into TAG. The second route involves FAs synthesized de novo during N-deprivation initially incorporated into membrane lipids, and their subsequent incorporation into TAG. The third route involves the incorporation of FAs synthesized de novo during N-deprivation directly into TAG. Our experiments show evidence for substantial flow through Route I. Evidence for substantial fluxes through Route II is explained above, in that PUFAs made during N-deprivation that accumulate in TAG were previously incorporated into a membrane lipid in order to be desaturated. However, our experiments cannot distinguish between Routes II and III for non-PUFA FAs (saturated, mono-, or di-unsaturated FAs), since for example C18:1 in TAG may have moved via MGDG as an intermediate (Route II) or through direct incorporation into TAG (Route III).

Membrane lipids contribute significantly to TAG accumulation

Prior isotopic labeling studies have made estimates of the relative contributions of de novo FA synthesis and membrane lipid recycling to TAG synthesis, suggesting that approximately 15%–25% of TAG is derived from preexisting

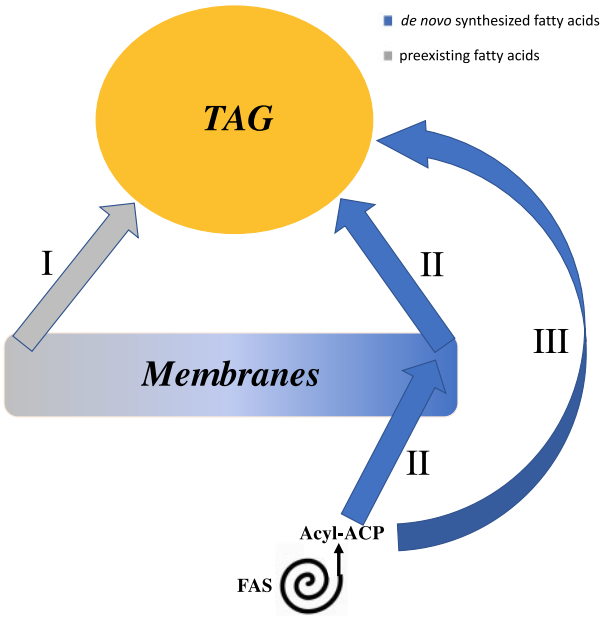

Figure 11 Diagram of the relationship between membrane lipids, TAG, and de novo FA synthesis during N-deprivation. Three different routes of FA flux into TAG during N-deprivation: (I) Preexisting membrane lipid acyl chains (synthesized prior to N-deprivation) are incorporated into TAG. (II) Acyl chains newly synthesized during N-deprivation are first esterified on membrane lipids prior to being incorporated into TAG, thus membrane lipids act as intermediates of FA flux into TAG. (III) FAs de novo synthesized during N-deprivation are incorporated directly into TAG.

membrane lipids, while 75%–85% of TAG is derived from de novo FA synthesis (Goncalves et al., 2013; Juergens et al., 2016; Allen et al., 2017). In our study, labeling with [1-^{14}C]- and [$^{13}C_2$]-acetate prior to N-deprivation (Figure 1A) allowed us to integrate the percentage of labeled FAs with quantities of FAs, thus showing that decreases in highly labeled PUFAs in membrane lipids account for the increases in highly labeled PUFAs in TAG during N-deprivation (Figure 7; Supplemental Figures S3, S4, and S8). Independently of labeling measurements, throughout the N-deprivation period, we observe based on FA composition that ~33% of TAG is composed of PUFAs (FAs with $\geqslant$3 double bonds), and these could be derived either from preexisting membrane lipids or from de novo synthesized FAs during N-deprivation which are incorporated into membrane lipids prior to accumulation in TAG (Routes I and II in Figure 11). We also observe that by 36 h of N-deprivation, ~10% of TAG was composed of highly labeled acyl chains that were not PUFAs (calculated from Figure 7A; Supplemental Figure S8), implying that ~10% of TAG was composed of saturated, mono-, or di-unsaturated FAs derived from preexisting membrane lipids. However, at the onset of N-deprivation, the FAs of membrane lipids were not fully ^{13}C-labeled, and taking this correction into consideration (under the assumption that labeled and unlabeled FAs are transferred in proportion to their abundance in the precursor pools), we conclude that ~12% of TAG FAs that were not PUFAs were derived from preexisting membrane lipids. Combined with the ~33% of TAG composed of PUFAs that originated in membrane lipids, we conclude that ~45% of the acyl chains in TAG are derived from membrane lipids, either passing through membrane lipids transiently during N-deprivation or from membrane lipids that were synthesized prior to N-deprivation. Based on the proportion of highly labeled acyl chains in TAG, ~35% of FAs in TAG are derived from preexisting membrane lipids made prior to N-deprivation. This is significantly higher than previous estimates of membrane lipid contributions to TAG synthesis, and indicates a significantly larger role of membranes in TAG accumulation than previously thought.

Multiple membrane lipid pools contribute different FAs to TAG synthesis

Previous studies have identified MGDG as the primary contributor of FAs to TAG accumulation under stress conditions (Urzica et al., 2013; Légeret et al., 2016), and recently a study has interpreted lipidomic measurements to indicate that DGDG and DGTS may be significant contributors to TAG accumulation as well (Yang et al., 2020). While we conclude that the galactolipids MGDG and DGDG have the largest contribution to TAG synthesis during N-deprivation, we also note that extraplastidial lipids contribute to TAG accumulation as well (Figure 5). This is supported by the fact that when the cells were prelabeled with [1-^{14}C]- and [$^{13}C_2$]-acetate prior to N-deprivation, highly labeled 18:3β (an FA diagnostic of extraplastidial membrane lipids) accumulated in TAG (Figure 7A). In addition, 18:3β in DGTS lost label during N-starvation and recovered its label during N-resupply (Figure 7C), suggesting that this FA is recycled between extraplastidial membrane lipids and TAG. Thus, although a biochemical mechanism for 18:1 acyl chain transfer from MGDG to TAG is known via the PGD1 lipase (Li et al., 2012a), there must be other mechanisms yet to be

characterized that conduct flux of acyl chains from both plastid and extraplastidial membrane lipids into TAG as well.

Our deductions from the results of the experiment in which cells were labeled during growth before N-deprivation (Figure 1A) are shown in Figure 12, with weighted arrows showing quantities of TAG FAs per culture volume, color designating the amount of ^{13}C label in each FA, and proposed origins of each FA are indicated with a bold or dashed border. PUFAs such as 16:4, 18:3α, and 18:3β contain high proportions of strongly labeled FAs, implying that much of the PUFA in TAG originated in preexisting membrane lipids. FAs with low levels of isotopic labeling, such as 18:1Δ9, are de novo synthesized during N-deprivation and may be incorporated into TAG directly or may be incorporated into membrane lipids during N-deprivation prior to their incorporation into TAG. 18:1Δ9 is incorporated into MGDG where it is rapidly desaturated to form 18:3α, and it has been previously reported that 18:1Δ9 is released from MGDG into TAG via the PDG1 lipase (Li et al., 2012a; Du et al., 2018). Flux of newly synthesized 18:1Δ9 through this small pool in MGDG resulted in very rapid replacement, as MGDG's 18:1Δ9 became almost entirely unlabeled immediately after transfer to the unlabeled, N-deprived medium in timecourse A (Supplemental Figure S9). Although 16:0 is a direct product of de novo FA synthesis and the majority of 16:0 in TAG was unlabeled, a significant quantity of 16:0 was highly labeled, suggesting that some 16:0 in TAG is derived from preexisting membrane lipids and some 16:0 is incorporated into TAG after de novo synthesis, possibly incorporated into membrane lipids before going into TAG. It should be noted that Figure 12 only indicates acyl fluxes, not the mechanisms by which the acyl chains are transferred to TAG. The FAs could be transferred to TAG via a lipase (Li et al., 2012a), a transacylase (Yoon et al., 2012), or by removal of the headgroup from a membrane lipid, forming DAG that acts as a precursor to TAG synthesis, as has been proposed previously (Légeret et al., 2016). In Figure 12, both plastidic and cytosolic DAG are shown to be utilized for TAG biosynthesis, as there are indications in the literature that chloroplast-derived DAG is used to produce TAG (Fan et al., 2011). Analysis of the composition of DAG FAs in timecourse A (Supplemental Figure S1G; Supplemental Table S1) revealed that DAG contains very low levels of 16:4. This strongly suggests that 16:4 does not make its way into TAG via conversion of MGDG to DAG by removal of the galactosyl headgroup followed by acylation to form TAG, as implied by Légeret et al. (2016). Rather, the absence of measurable levels of 16:4 in DAG indicates that this FA is removed from MGDG and transferred to TAG via the action of a lipase or transacylase. Subcellular fractionation would be required to analyze the cytosolic versus plastidic DAG pools in order to assign pathways of flux through the different DAG pools, and further experiments involving

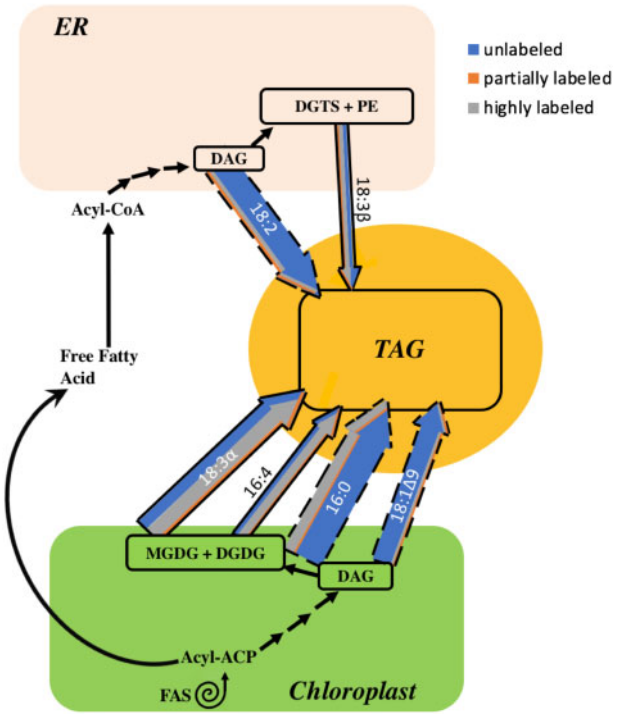

Figure 12 Acyl chain flux into TAG during N-deprivation in timecourse A. Membrane lipid and de novo FA synthesis contribution to TAG accumulation during N-deprivation. Colored arrows represent acyl chain fluxes into TAG at 36 h of N-deprivation after labeled acetate was applied during N-replete growth (Figure 1A). Arrow weights are based on the quantity of each FA and divided into low, intermediate, and high levels of labeling based on the isotopic label distribution of each FA in TAG. FAs whose origins are more certain are shown with a bold border, while those whose origins are less clear are shown with a dashed border. Black arrows indicate routes of fatty acyl chain movement without indicating relative quantities, sequential black arrows indicate multi-step pathways.

stereochemical and intact lipid analyses will be required to gain insight as to the mechanism of acyl transfer from membrane lipids to TAG.

In land plants, a significant contribution to TAG synthesis is made by newly synthesized FAs being directly incorporated into the lipid phosphatidylcholine (PC), where desaturation takes place in seeds and developing embryos (Bates et al., 2009; Bates and Browse, 2011). *Chlamydomonas reinhardtii* does not contain PC, and the PC acyl editing cycle depends on the enzyme lysophosphatidylcholine acyltransferase deacylating and reacylating PC (Stymne and Stobart, 1984), and the conversion of PC to DAG via the enzymes CDP-choline:1,2-diacylglycerol cholinephosphotransferase (Slack et al., 1983) and PC:diacylglycerol cholinephosphotransferase (Lu et al., 2009). It is suspected that the betaine lipid DGTS replaces the function of PC in *C. reinhardtii*, but analogous enzymes providing similar functions on DGTS rather than PC have yet to be characterized in *C. reinhardtii*. In addition, although there is well-known transfer of an acyl group from a phospholipid such as PC onto DAG to form TAG via the enzyme PDAT in land plants (Dahlqvist et al., 2000), *C. reinhardtii's* PDAT enzyme has been shown to possess broad substrate specificities in in vitro assays (Yoon et al., 2012). PDAT knockdown mutants in *C. reinhardtii* had statistically insignificant differences in their maximum TAG accumulation under N-deprivation compare to wild-type, suggesting that the contribution of the PDAT pathway to TAG synthesis is minor in *C. reinhardtii* (Yoon et al., 2012). Thus, it is not yet known if the well-characterized paradigm of PC acyl editing has an analogous system in *C. reinhardtii*.

TAG contributes much of the FA for membranes synthesized during recovery from N-deprivation

Previous work has indicated that TAG contributes acyl chains to galactolipid resynthesis during N-resupply (Khozin-Goldberg et al., 2005; Allen et al., 2015), but the proportion of membrane lipid synthesis that this flux represents has not been estimated. By labeling with [1-^{14}C]- and [$^{13}C_2$]-acetate during N-deprivation and chasing with unlabeled N-replete medium (Figure 1B), we found that 63% of the increase in membrane lipid acyl chains by 12 h of N-resupply represented the influx of highly labeled FA molecules from TAG (Figure 9; Supplemental Figure S10). As N-resupply continues, during the period from 12 to 24 h of N-resupply 46% of the increase in membrane lipid acyl chains came from highly labeled FAs, and from 24 to 36 h of N-resupply (after the resumption of N-replete growth rates) only 8.2% of the increase in membrane lipid acyl chains was from highly labeled FAs. Thus, there is a dramatic drop in the contribution of TAG acyl chains to membrane lipids as TAG levels are depleted, after which de novo FA synthesis takes over as the primary contributor to new membrane synthesis. In addition, we note that galactolipids are not the sole recipients of highly labeled acyl chains from TAG, as we also observe radiolabel and highly labeled FAs increase in extraplastidial lipids as well (Figures 6 and 9). The results of this experiment (Figure 1B) are shown in Figure 13, which also uses weighted and colored arrows to represent quantities and label distribution of FAs in membrane lipids during N-resupply. During the early regrowth phase of N-resupply (up to 12 h N-resupply), highly labeled acyl chains from TAG contribute strongly to membrane lipid synthesis as shown by the colored arrows, while later in N-resupply de novo FA synthesis contributes more strongly to membrane lipid resynthesis, as shown by black arrows.

If the highly labeled FAs in TAG were first undergoing β-oxidation to acetyl-CoA and then FA synthesis to form new membrane lipid FAs, we would observe an increase in partially labeled FAs in membrane lipids during N-resupply due to ^{13}C-acetyl-CoA mixing with unlabeled acetyl-CoA during FA synthesis. Most of the membrane lipid FAs showed little increase in partially labeled molecules, and only a few showed substantial increases in partial labeling (Figure 9; Supplemental Figure S10). Rather, we observe evidence of transfer of intact acyl chains from TAG into membrane lipids during N-resupply. For example, we observe an increase in highly labeled MGDG 18:1Δ9 during N-resupply followed by an increase in highly labeled MGDG 18:2 (Supplemental Figure S10), suggesting a precursor–product relationship between these FAs. This implies that highly labeled saturated and mono-unsaturated C18s from TAG are transferred to MGDG and desaturated to form 18:2 followed by 18:3α. However, these quantities are not high enough to fully explain the large rise in highly labeled 18:3α in MGDG during N-resupply (Figure 9), suggesting that a large amount of 18:3α is transferred intact from TAG to MGDG. In addition, the decrease in highly labeled 16:0 in TAG during N-resupply (Figure 8; Supplemental Figure S2) is greater than the increase in highly labeled 16:0 in membrane lipids (Figure 9; Supplemental Figure S10), while the increase in highly labeled C16 PUFAs in membrane lipids is larger than the decrease in their levels in TAG. This strongly implies that some of the highly labeled 16:0 in TAG that is transferred to membrane lipids is desaturated to form 16:3 and 16:4 that are found predominantly in glycolipids. Thus, the isotopic labeling distribution in membrane lipid FAs during N-resupply indicates that intact transfer of highly labeled FAs from TAG to membrane lipids during N-resupply is a much more important contributor than β-oxidation of TAG FAs followed by resynthesis.

Prior transcript studies note that several putative lipase genes displayed increased mRNA abundance in the early phase of N-deprivation (Gargouri et al., 2015), and that the mRNA levels of FA biosynthesis components were reduced earlier in N-deprivation, recovering later in N-deprivation (Schmollinger et al., 2014). These findings suggest that membrane lipid recycling into TAG may play a more prominent role earlier in N-deprivation, with de novo FA synthesis becoming more prominent in later stages of N-deprivation. However, when cells were labeled with [1-^{14}C]- and [$^{13}C_2$]-acetate prior to N-deprivation (Figure 1A), we observed that the rise in highly labeled FAs in TAG during N-deprivation was not limited to the early stage of N-deprivation, but

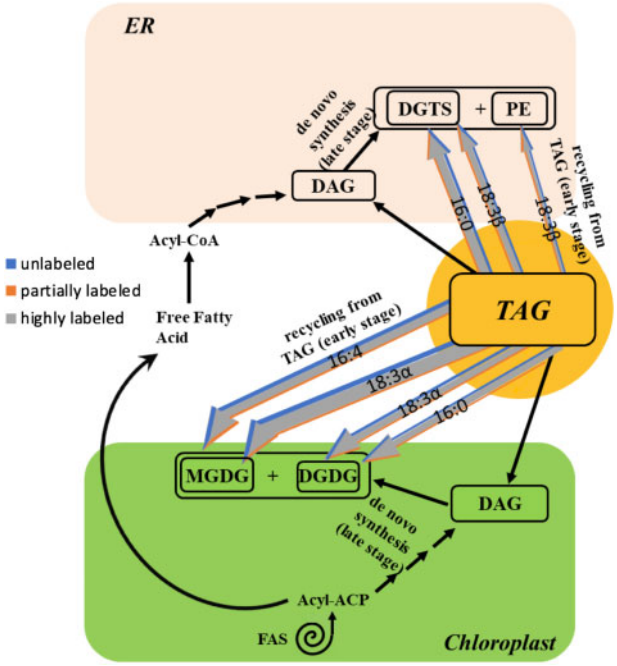

Figure 13 Acyl chain flux into membrane lipids during N-resupply in timecourse B. Triacylglycerol TAG and de novo FA synthesis contribution to membrane lipids during early and late N-resupply, respectively. Colored arrows represent acyl chain remodeling from TAG into membrane lipids at 12 h of N-resupply after labeled acetate was supplied during N-deprivation (Figure 1B). Arrow weights are based on the quantity of each FA and divided into low, intermediate, and high levels of labeling based on the isotopic label distribution of each FA in membrane lipids. De novo FA synthesis contributes significantly to membrane lipid synthesis in later stages of N-resupply when TAG has been depleted. Black arrows indicate routes of fatty acyl chain movement without indicating relative quantities and sequential black arrows indicate multi-step pathways.

rather was linear throughout the entire 72-h N-deprivation period (Supplemental Figure S8). Thus, the flux of FAs from membrane lipids into TAG is not limited to the early stage of N-deprivation. Similarly, Allen et al. (2017) concluded that in *C. subellipsoidea* the contribution of preexisting membrane lipids to TAG continued beyond the early stages of TAG accumulation. The persistence of label incorporation from membrane lipids into TAG demonstrates that dynamic recycling of membrane lipids into TAG occurs throughout the entire N-deprivation period.

A storage role for TAG accumulation

The primary physiological function of TAG accumulation (i.e. its adaptive benefit) is generally believed to be to prevent over-reduction of the photosynthetic electron transport chain and subsequent photooxidative damage by serving as a sink for photosynthetic reductant and fixed carbon when growth is inhibited (Hu et al., 2008). Although there have been reports that some preexisting acyl chains in membrane lipids move to TAG during N-deprivation (Simionato et al., 2013; Allen et al., 2015) and that TAG supplies some of the FAs for the synthesis of membrane lipids when growth resumes (Khozin-Goldberg et al., 2005), the prevailing view that TAG is synthesized largely from de novo FA biosynthesis during N-deprivation (Fan et al., 2011) suggests that TAG's role as an intracellular storage pool is secondary. Our findings here (Figures 5 and 7) demonstrate that a higher proportion of TAG is derived from preexisting membrane lipids than previously reported, with ~35% of FAs in TAG derived from preexisting membrane lipids made prior to N-deprivation. In addition, the results demonstrate that during the early phase of N-resupply, the majority of new membrane lipid synthesis comes from acyl chains derived from TAG (Figure 9). These results quantify and highlight TAG's role in storing and resupplying FAs to membrane lipids during N-deprivation and resupply, and could help explain why mutants impaired in TAG breakdown are also impaired in their resynthesis of membrane lipids during N-resupply (Tsai et al., 2018; Warakanont et al., 2019).

Through experiments using two isotopic labeling schemes, we have contributed to answering the questions outlined in the introduction pertaining to the relationship between TAG and membrane lipids during nutrient deprivation and resupply: (1) concerning the contribution of membrane lipids to TAG synthesis during N-deprivation, based on the proportion of highly labeled acyl chains in TAG, ~35% of TAG is composed of FAs from preexisting membrane lipids. When taking into account that PUFAs in TAG that were de novo synthesized during N-deprivation must have previously been incorporated in a membrane lipid in order to be desaturated, we find that ~45% of the FAs in TAG were previously in membrane lipids at some point, whether prior to or during N-deprivation; (2) concerning which polar lipid FAs contribute significantly to TAG, PUFAs comprise 64% of the TAG FAs that are derived from preexisting membrane lipids

(Figure 7A, Supplemental Figure S8); (3) concerning the extent of membrane lipid turnover during N-deprivation, we found that 84% of the membrane lipid FAs were largely or entirely replaced within 72 h of N-deprivation; (4) concerning the fate of FAs in TAG during N-resupply, we determined that 63% of new membrane synthesis in the initial 12 h of N-resupply represented highly labeled FA molecules derived from TAG (Figure 9; Supplemental Figure S10), with de novo FA synthesis driving the majority of new membrane synthesis as TAG levels are depleted; and (5) by analyzing ^{13}C-labeling in starch and proteins, we determined that these biomass components contribute little to new membrane lipid synthesis during N-resupply, concluding that FAs resulting from TAG breakdown supply the majority of the carbon for membrane lipid resynthesis when growth resumes upon nutrient resupply.

In addition, using ^{14}C-labeling, we found that the carbon accumulated in TAG is retained in cellular lipids throughout the N-resupply period while TAG is fully degraded (Figure 4, A and B), which supports the role of TAG as a storage pool. Although previous studies had provided evidence for membrane lipid contributions to TAG synthesis, the fluxes identified here are larger and more detailed than previously demonstrated. To address the mechanisms behind the fluxes identified in this work, future studies should analyze labeling stereospecificity, labeling in whole lipid molecules, and labeling in the glycerol backbones versus the acyl chains. In addition, it would be of interest to conduct future studies under a range of ecologically relevant growth conditions (Sasso et al., 2018). However, it is clear from this work that TAG and membrane lipids have a close relationship both mechanistically and functionally, with multiple routes of FA transfer operating during N-deprivation and N-resupply. The large fluxes through these routes justify a reconsideration of the adaptive reasons that algal cells accumulate TAG under stress conditions. While other work has provided evidence for this, our use of ^{14}C- and ^{13}C-labeling allowed us to quantify the exchange of acyl chains between TAG and membrane lipids during nutrient deprivation and resupply, demonstrating that TAG and membrane lipids are more intimately linked pools than was hitherto known.

Materials and methods

Strain and culture conditions

Chlamydomonas reinhardtii strain cc400 cw-15 mt+ was obtained from the Chlamydomonas Resource Center and grown in batch cultures at 24°C in 250 mL TAP medium with Hutner trace elements (Gorman and Levine, 1965) in 1-L flasks shaken at 136 rpm under continuous illumination at 160 µmol photons m^{-2} s^{-1} and ambient CO_2 concentrations. Cell growth was determined by OD measurements at 750 nm using a DU 800 spectrophotometer (Beckman Coulter, Brea, CA, USA). Cells were counted during time-course experiments using a hemocytometer. For chlorophyll measurement, 1 mL of cells were pelleted by centrifugation, supernatant was removed, and chlorophyll was extracted in 1 mL of 3:2 acetone:Dimethyl sulfoxide. After extraction, samples were pelleted by centrifugation and the supernatant was used to quantify chlorophyll spectroscopically as described (Ritchie, 2006) by measuring absorbance at 646 and 663 nm using a DU 800 spectrophotometer (Beckman Coulter).

Labeling prior to N-deprivation

Cultures were grown in TAP medium containing 100% uniformly labeled ^{13}C acetate as well as 100 µCi of ^{14}C acetate to cell densities between 0.2 and 0.3 OD_{750} prior to N-deprivation to minimize self-shading, which becomes significant at densities >0.3. In all experiments, cell densities were kept below OD_{750} of 0.3 by dilution when necessary. For N-deprivation, cells were centrifuged and supernatant media was carefully removed from the pellet using a pipette. A wash step was performed using TAP medium lacking ammonium chloride (the N source) in order to fully remove N, after which cells were resuspended in TAP-N medium. Cells were cultured in TAP-N medium for 72 h, after which they were centrifuged, the supernatant removed, and cells were resuspended in TAP medium for 36 h of N-resupply (Figure 1A).

Labeling during N-deprivation

Cultures were grown in TAP medium to cell densities between 0.2 and 0.3 OD_{750} prior to N-deprivation. For N-deprivation, cells were centrifuged, supernatant was removed, a wash step was performed using TAP-N medium, after which cells were resuspended in TAP-N medium containing 100% uniformly labeled ^{13}C acetate as well as 100 µCi of ^{14}C acetate. Cells were cultured for 68 h in N-deprivation, after which they were centrifuged, the supernatant removed, and cells were resuspended in TAP medium for N-resupply for 48 h (Figure 1B).

Lipid extraction

Cells were harvested by centrifugation and total lipids were extracted by the method of Folch et al. (1957). Briefly, cells were extracted with 1.5 mL of $CHCl_3$:MeOH (1:2, v/v), and samples were vortexed to resuspend the pellet. The samples were then centrifuged and the supernatant collected; the extraction was repeated and the supernatant extracts were pooled. To the extract, 0.5 volume of 1 M KCl and 0.2 M H_3PO_4 was added, the sample was mixed, and organic and aqueous phases were separated by centrifugation. The upper phase was removed, and the lower phase was collected and dried under flowing N_2 gas at room temperature and stored at −20°C until further analysis.

Separation of lipids on TLC plates

Total lipid extracts were loaded on Analtech uniplate silica gel HL plates (Analtech, Newark, Delaware), and neutral lipids were resolved by development in toluene:chloroform:methanol (85:15:5 v/v). Polar lipids were resolved on a separate TLC plate by development in chloroform:methanol:acetic acid:water (75:13:9:3 v/v).

Recovery of lipids from TLC plate

Lipids were visualized on the TLC plate by spraying with a 0.01% (v/v) primuline solution dissolved in acetone/water (80/20, v/v), after which bands of individual lipid classes were separately scraped off the TLC plate. The recovered silica powder was loaded onto a glass Pasteur pipette containing ~2–4 mm of glass wool at the bottom. Then 4 mL of $CHCl_3$:MeOH:H_2O (5:5:1 v/v) was used to elute polar lipids from the silica, while 4 mL of $CHCl_3$:MeOH (2:1 v/v) was used to elute neutral lipids. To the eluate, 2 mL of chloroform and 2 mL of 0.9% (w/v) KCl was added and mixed, and the phases were separated by centrifugation. The upper phase was removed, and the lower phase was collected and dried under flowing N_2 gas at room temperature and stored at −20°C.

Fatty acyl transesterification

Total lipid extracts were treated with 200 µL 2 M methanolic KOH in 1 mL hexane and vortexed for 2 min at room temperature. Then, 200 µL of 3N HCl was added to neutralize the pH, samples were vortexed briefly, and centrifuged. The upper hexane phase was transferred to another glass tube and then dried under flowing N_2 gas at room temperature. Samples were resuspended in 200 µL of heptane and quantified using an Agilent 6890N GC-FID with a 1:10 split injection at 250°C, oven temperature ramp from 140°C to 230°C at 10°C/min on a DB-23 capillary column (30 m × 0.25 mm id, 0.25-μm film thickness).

Starch analyses

Total glucose contained in starch was measured after amyloglucosidase and amylase digestion with the Megazyme total starch analysis kit as described in Juergens et al. (2016). Briefly, pellets remaining after extraction of lipids from cells were autoclaved for 1 h in 0.1 M acetate buffer, pH 4.8, then treated with α-amylase and amyloglucosidase for 1 h at 55°C. Free glucose was quantitated with a colorimetric assay at 510 nm using a starch assay kit (Megazyme, Bray, Ireland) according to the manufacturer's instructions. Starch hydrolyzed to glucose was incubated in 100 µL of a 20 mg/mL methoxyamine HCl in pyridine solution for 30 min at 60°C, followed by trimethylsilyl (Sigma, St Louis, MO, USA) derivatization (Roessner et al., 2001). Labeling was then analyzed on a Thermo TRACE GC Ultra using a VF5 column.

Protein analyses

Proteins were extracted from pellets remaining after extraction of lipids using 20 mM Tris–HCl, pH 7.5; 150 mM NaCl; and 1% sodium dodecyl sulfate buffer at 42°C. Extracted proteins were hydrolyzed to amino acids in 6 M HCl at 120°C for 3 h, and then purified using a cation exchange column of dowex as previously described (Carey et al., 2020). Purified amino acids were derivatized for GC–MS analysis using *N*-tert-butyldimethylsilyl-*N*-methyltrifluoroacetamide + 1% tert-Butyldimethylchlorosilane (Dauner and Sauer, 2000), and samples were run on a Thermo TRACE GC Ultra using a VF5 column.

^{14}C FAME analysis

FAMEs resulting from transmethylated total lipid extracts and transmethylated lipids eluted from TLC plates were assayed for radioactivity by liquid scintillation counting using a PerkinElmer MicroBeta TriLux 1450 LSC & Luminescence Counter.

GC–MS of FAMEs

For the experiment outlined in Figure 1B, FAMEs were analyzed by an Agilent 7890B GC System using a 7010B triple quadrupole GC–MS in chemical ionization (CI) mode. FAMEs were separated on a DB-23 column using splitless injection at 250°C and an oven temperature ramp from 160°C to 210°C at 3°C/min, followed by a final ramp of 40°C/min to 250°C and a 3 min hold. The carrier gas used was helium.

For the experiment outlined in Figure 1A, FAMEs were analyzed by a Thermo TRACE GC Ultra and DSQII single quadrupole MS in CI mode. FAMEs were separated on a DB-23 column using a 1:10 split ratio, injected at 250°C, and an oven temperature ramp from 160°C to 210°C at 3°C/min, followed by a final ramp of 40°C/min to 250°C and a 3 min hold. The carrier gas used was helium.

Replication and statistical analyses

Three replicate cultures were grown for each experimental timecourse, which were conducted as separate, independent experiments, and the three replicate cultures were sampled at successive timepoints. In each figure, error bars indicate ±standard deviation (SD) of three biological replicate cultures.

Supplemental data

The following materials are available in the online version of this article.

Supplemental Figure S1 FA contents of individual lipids during N-starvation and N-resupply (Figure 1A).

Supplemental Figure S2 Quantity of FAs in TAG during N-resupply (Figure 1B), divided into low, intermediate, and high levels of ^{13}C-acetate incorporation.

Supplemental Figure S3 Quantity of major FAs in membrane lipid classes and DAG during N-deprivation and N-resupply (Figure 1A), divided into low, intermediate, and high levels of ^{13}C-acetate incorporation.

Supplemental Figure S4 Quantity of minor FAs in membrane lipid classes during N-deprivation and N-resupply (Figure 1A), divided into low, intermediate, and high levels of ^{13}C-acetate incorporation.

Supplemental Figure S5 Starch quantity during each experimental timecourse.

Supplemental Figure S6 ^{13}C isotopomer distribution of amino acids at the end of the N-deprivation labeling period (Figure 1B).

Supplemental Figure S7 ^{13}C isotopomer distribution of FAMEs in membrane lipids and TAG during N-resupply (Figure 1B).

Supplemental Figure S8 Quantity of FAs in TAG during N-starvation and N-resupply (Figure 1A), divided into low, intermediate, and high levels of ^{13}C-acetate incorporation.

Supplemental Figure S9 ^{13}C isotopomer distribution of 18:1Δ9 in MGDG just before and just after transfer to unlabeled, N-deprived medium in timecourse A.

Supplemental Figure S10 Quantity of FAs in membrane lipid classes during N-resupply (Figure 1B) divided into low, intermediate, and high levels of ^{13}C-acetate incorporation.

Supplemental Table S1 Relative abundance of FAs in major lipid classes during log growth, N-deprivation, and N-resupply

Acknowledgments

The authors gratefully thank Dr Cassandra Johnny of the Michigan State University Research Technology Support Facility Mass Spectrometry & Metabolomics Core for GC–MS technical support and instrumentation.

Funding

This work was supported by the National Institute of General Medical Sciences of the National Institutes of Health pre-doctoral training award from grant no. T32-GM110523 to D.Y.Y. Its contents are solely the responsibility of the authors and do not necessarily represent the official views of the NIGMS or NIH. Research in the Shachar-Hill lab is supported by the US Department of Energy (Biological and Environmental Research grant no. DE-SC0018269).

Conflict of interest statement. The authors declare no conflict of interest.

References

Allen JW, DiRusso CC, Black PN (2015) Triacylglycerol synthesis during nitrogen stress involves the prokaryotic lipid synthesis pathway and acyl chain remodeling in the microalgae *Coccomyxa subellipsoidea*. Algal Res **10**: 110–120

Allen JW, DiRusso CC, Black PN (2017) Carbon and acyl chain flux during stress-induced triglyceride accumulation by stable isotopic labeling of the polar microalga *Coccomyxa subellipsoidea* C169. J Biol Chem **292:** 361–374

Bates PD, Durrett TP, Ohlrogge JB, Pollard M (2009) Analysis of acyl fluxes through multiple pathways of triacylglycerol synthesis in developing soybean embryos. Plant Physiol **150:** 55–72

Bates PD, Browse J (2011) The pathway of triacylglycerol synthesis through phosphatidylcholine in *Arabidopsis* produces a bottleneck for the accumulation of unusual fatty acids in transgenic seeds. Plant J **68:** 387–399

Carey LM, Clark TJ, Deshpande RR, Cocuron JC, Rustad EK, Shachar-Hill Y (2020) High flux through the oxidative pentose phosphate pathway lowers efficiency in developing Camelina seeds. Plant Physiol **182:** 493–506

Chisti Y (2007) Biodiesel from microalgae. Biotechnol Adv **25:** 294–306

Dahlqvist A, Ståhl U, Lenman M, Banas A, Lee M, Sandager L, Ronne H, Stymne S (2000) Phospholipid: diacylglycerol acyltransferase: an enzyme that catalyzes the acyl-CoA-independent formation of triacylglycerol in yeast and plants. Proc Natl Acad Sci USA **97:** 6487–6492

Dauner M, Sauer U (2000) GC-MS analysis of amino acids rapidly provides rich information for isotopomer balancing. Biotechnol Prog **16:** 642–649

Du ZY, Lucker BF, Zienkiewicz K, Miller TE, Zienkiewicz A, Sears BB, Kramer DM, Benning C (2018) Galactoglycerolipid lipase PGD1 is involved in thylakoid membrane remodeling in response to adverse environmental conditions in *Chlamydomonas*. Plant Cell **30:** 447–465

Durrett TP, Benning C, Ohlrogge J (2008) Plant triacylglycerols as feedstocks for the production of biofuels. Plant J **54:** 593–607

Eccleston VS, Ohlrogge JB (1998) Expression of lauroyl–acyl carrier protein thioesterase in *Brassica napus* seeds induces pathways for both fatty acid oxidation and biosynthesis and implies a set point for triacylglycerol accumulation. Plant Cell **10:** 613–621

Fan J, Andre C, Xu C (2011) A chloroplast pathway for the *de novo* biosynthesis of triacylglycerol in *Chlamydomonas reinhardtii*. FEBS Lett **585:** 1985–1991

Folch J, Lees M, Stanley GS (1957) A simple method for the isolation and purification of total lipides from animal tissues. J Biol Chem **226:** 497–509

Gargouri M, Park JJ, Holguin FO, Kim MJ, Wang H, Deshpande RR, Shachar-Hill Y, Hicks LM, Gang DR (2015) Identification of regulatory network hubs that control lipid metabolism in *Chlamydomonas reinhardtii*. J Exp Bot **66:** 4551–4566

Giroud C, Eichenberger W (1989) Lipids of *Chlamydomonas reinhardtii*. Incorporation of [14C] acetate,[14C] palmitate and [14C] oleate into different lipids and evidence for lipid-linked desaturation of fatty acids. Plant Cell Physiol **30:** 121–128

Goncalves EC, Johnson JV, Rathinasabapathi B (2013) Conversion of membrane lipid acyl groups to triacylglycerol and formation of lipid bodies upon nitrogen starvation in biofuel green algae *Chlorella* UTEX29. Planta **238:** 895–906

Goodson C, Roth R, Wang ZT, Goodenough U (2011) Structural correlates of cytoplasmic and chloroplast lipid body synthesis in *Chlamydomonas reinhardtii* and stimulation of lipid body production with acetate boost. Eukaryot Cell **10:** 1592–1606

Goold HD, Cuiné S, Légeret B, Liang Y, Brugière S, Auroy P, Javot H, Tardif M, Jones B, Beisson F, et al. (2016) Saturating light induces sustained accumulation of oil in plastidal lipid droplets in *Chlamydomonas reinhardtii*. Plant Physiol **171:** 2406–2417

Gorman DS, Levine RP (1965) TAP and Tris-minimal medium recipes. Proc Natl Acad Sci USA **54:** 1665–1669

Hannon M, Gimpel J, Tran M, Rasala B, Mayfield S (2010) Biofuels from algae: challenges and potential. Biofuels **1:** 763–784

Harris EH (2001) *Chlamydomonas* as a model organism. Annu Rev Plant Biol **52:** 363–406.

Harris EH (2009) The Chlamydomonas Sourcebook: Introduction to Chlamydomonas and its Laboratory Use, Vol **1**. Academic Press, Oxford

Höök M, Tang X (2013) Depletion of fossil fuels and anthropogenic climate change—A review. Energy policy **52:** 797–809

Hu Q, Sommerfeld M, Jarvis E, Ghirardi M, Posewitz M, Seibert M, Darzins A (2008) Microalgal triacylglycerols as feedstocks for biofuel production: perspectives and advances. Plant J **54:** 621–639

Janssen JH, Lamers PP, de Vos RC, Wijffels RH, Barbosa MJ (2019) Translocation and *de novo* synthesis of eicosapentaenoic acid (EPA) during nitrogen starvation in *Nannochloropsis gaditana*. Algal Res **37:** 138–144

Jinkerson RE, Jonikas MC (2015) Molecular techniques to interrogate and edit the *Chlamydomonas* nuclear genome. Plant J **82:** 393–412

Juergens MT, Disbrow B, Shachar-Hill Y (2016) The relationship of triacylglycerol and starch accumulation to carbon and energy flows during nutrient deprivation in *Chlamydomonas reinhardtii*. Plant Physiol **171:** 2445–2457

Khozin-Goldberg I, Shrestha P, Cohen Z (2005) Mobilization of arachidonyl moieties from triacylglycerols into chloroplastic lipids

following recovery from nitrogen starvation of the microalga *Parietochloris incisa*. Biochim Biophys Acta **1738:** 63–71

Lee DY, Park JJ, Barupal DK, Fiehn O (2012) System response of metabolic networks in *Chlamydomonas reinhardtii* to total available ammonium. Mol Cell Proteomics **11:** 973–988

Légeret B, Schulz-Raffelt M, Nguyen HM, Auroy P, Beisson F, Peltier G, Blanc G, Li-Beisson Y (2016) Lipidomic and transcriptomic analyses of *Chlamydomonas reinhardtii* under heat stress unveil a direct route for the conversion of membrane lipids into storage lipids. Plant Cell Environ **39:** 834–847

Li X, Moellering ER, Liu B, Johnny C, Fedewa M, Sears BB, Kuo MH, Benning C (2012a) A galactoglycerolipid lipase is required for triacylglycerol accumulation and survival following nitrogen deprivation in *Chlamydomonas reinhardtii*. Plant Cell **24:** 4670–4686

Li X, Benning C, Kuo MH (2012b) Rapid triacylglycerol turnover in *Chlamydomonas reinhardtii* requires a lipase with broad substrate specificity. Eukaryot Cell **11:** 1451–1462

Li-Beisson Y, Beisson F, Riekhof W (2015) Metabolism of acyl-lipids in *Chlamydomonas reinhardtii*. Plant J **82:** 504–522

Livne A, Sukenik A (1992) Lipid synthesis and abundance of acetyl CoA carboxylase in *Isochrysis galbana* (Prymnesiophyceae) following nitrogen starvation. Plant Cell Physiol **33:** 1175–1181

Lu C, Xin Z, Ren Z, Miquel M (2009) An enzyme regulating triacylglycerol composition is encoded by the ROD1 gene of *Arabidopsis*. Proc Natl Acad Sci USA **106:** 18837–18842

Merchant SS, Prochnik SE, Vallon O, Harris EH, Karpowicz SJ, Witman GB, Terry A, Salamov A, Fritz-Laylin L, Maréchal-Drouard L, et al. (2007) The *Chlamydomonas* genome reveals the evolution of key animal and plant functions. Science **318:** 245–250

Miller R, Wu G, Deshpande RR, Vieler A, Gärtner K, Li X, Moellering ER, Zäuner S, Cornish AJ, Liu B, et al. (2010) Changes in transcript abundance in *Chlamydomonas reinhardtii* following nitrogen deprivation predict diversion of metabolism. Plant Physiol **154:** 1737–1752

Moellering ER, Miller R, Benning C (2009) Molecular genetics of lipid metabolism in the model green alga *Chlamydomonas reinhardtii*. Lipids in Photosynthesis, Advances in Photosynthesis and Respiration, Vol **30**. Springer Netherlands, Dordrecht, Netherlands, pp. 139–155

Moellering ER, Benning C (2010) RNA interference silencing of a major lipid droplet protein affects lipid droplet size in *Chlamydomonas reinhardtii*. Eukaryot Cell **9:** 97–106

Moriyama T, Toyoshima M, Saito M, Wada H, Sato N (2018) Revisiting the algal "chloroplast lipid droplet": the absence of an entity that is unlikely to exist. Plant Physiol **176:** 1519–1530

Msanne J, Xu D, Konda AR, Casas-Mollano JA, Awada T, Cahoon EB, Cerutti H (2012) Metabolic and gene expression changes triggered by nitrogen deprivation in the photoautotrophically grown microalgae *Chlamydomonas reinhardtii* and *Coccomyxa* sp. C-169. Phytochemistry **75:** 50–59

Mussgnug JH (2015) Genetic tools and techniques for *Chlamydomonas reinhardtii*. Appl Microbiol Biotechnol **99:** 5407–5418

Pick U, Avidan O (2017) Triacylglycerol is produced from starch and polar lipids in the green alga *Dunaliella tertiolecta*. J Exp Bot **68:** 4939–4950

Ritchie RJ (2006) Consistent sets of spectrophotometric chlorophyll equations for acetone, methanol and ethanol solvents. Photosynth Res **89:** 27–41

Roessner U, Luedemann A, Brust D, Fiehn O, Linke T, Willmitzer L, Fernie AR (2001) Metabolic profiling allows comprehensive phenotyping of genetically or environmentally modified plant systems. Plant Cell **13:** 11–29

Sasso S, Stibor H, Mittag M, Grossman AR (2018) The natural history of model organisms: from molecular manipulation of domesticated *Chlamydomonas reinhardtii* to survival in nature. eLife **7**: e39233

Schmollinger S, Mühlhaus T, Boyle NR, Blaby IK, Casero D, Mettler T, Moseley JL, Kropat J, Sommer F, Strenkert D, et al. (2014) Nitrogen-sparing mechanisms in *Chlamydomonas* affect the transcriptome, the proteome, and photosynthetic metabolism. Plant Cell **26:** 1410–1435

Scranton MA, Ostrand JT, Fields FJ, Mayfield SP (2015). *Chlamydomonas* as a model for biofuels and bio-products production. Plant J **82:** 523–531

Shifrin NS, Chisholm SW (1981) Phytoplankton lipids: interspecific differences and effects of nitrate, silicate and light-dark cycles. J Phycol **17:** 374–384

Siaut M, Cuiné S, Cagnon C, Fessler B, Nguyen M, Carrier P, Beyley A, Beisson F, Triantaphylidès C, Li-Beisson Y, Peltier G (2011) Oil accumulation in the model green alga *Chlamydomonas reinhardtii*: characterization, variability between common laboratory strains and relationship with starch reserves. BMC Biotechnol **11:** 7

Simionato D, Block MA, La Rocca N, Jouhet J, Maréchal E, Finazzi G, Morosinotto T (2013) The response of *Nannochloropsis gaditana* to nitrogen starvation includes *de novo* biosynthesis of triacylglycerols, a decrease of chloroplast galactolipids, and reorganization of the photosynthetic apparatus. Eukaryot Cell **12:** 665–676

Slack CR, Campbell LC, Browse JA, Roughan PG (1983) Some evidence for the reversibility of the cholinephosphotransferasecatalysed reaction in developing linseed cotyledons in vivo. Biochim Biophys Acta **754:** 10–20

Stymne S, Stobart AK (1984) Evidence for the reversibility of the acyl-CoA: lysophosphatidylcholine acyltransferase in microsomal preparations from developing safflower (*Carthamus tinctorius* L.) cotyledons and rat liver. Biochem J **223:** 305–314

Tsai CH, Warakanont J, Takeuchi T, Sears BB, Moellering ER, Benning C (2014) The protein Compromised Hydrolysis of Triacylglycerols 7 (CHT7) acts as a repressor of cellular quiescence in *Chlamydomonas*. Proc Natl Acad Sci USA **111:** 15833–15838

Tsai CH, Uygun S, Roston R, Shiu SH, Benning C (2018) Recovery from N deprivation is a transcriptionally and functionally distinct state in *Chlamydomonas*. Plant Physiol **176:** 2007–2023

Urzica EI, Vieler A, Hong-Hermesdorf A, Page MD, Casero D, Gallaher SD, Kropat J, Pellegrini M, Benning C, Merchant SS (2013) Remodeling of membrane lipids in iron-starved *Chlamydomonas*. J Biol Chem **288:** 30246–30258

Warakanont J, Li-Beisson Y, Benning C (2019) LIP4 Is Involved in Triacylglycerol Degradation in *Chlamydomonas reinhardtii*. Plant Cell Physiol **60:** 1250–1259

Work VH, Radakovits R, Jinkerson RE, Meuser JE, Elliott LG, Vinyard DJ, Laurens LML, Dismukes GC, Posewitz MC (2010) Increased lipid accumulation in the *Chlamydomonas reinhardtii sta7-10* starchless isoamylase mutant and increased carbohydrate synthesis in complemented strains. Eukaryot Cell **9:** 1251–1261

Yang M, Kong F, Xie X, Wu P, Chu Y, Cao X, Xue S (2020) Galactolipid DGDG and Betaine Lipid DGTS Direct *De novo* Synthesized Linolenate into Triacylglycerol in a Stress-Induced Starchless Mutant of *Chlamydomonas reinhardtii*. Plant Cell Physiol **61:** 851–862

Yoon K, Han D, Li Y, Sommerfeld M, Hu Q (2012) Phospholipid: diacylglycerol acyltransferase is a multifunctional enzyme involved in membrane lipid turnover and degradation while synthesizing triacylglycerol in the unicellular green microalga *Chlamydomonas reinhardtii*. Plant Cell **24:** 3708–3724

Zäuner S, Jochum W, Bigorowski T, Benning C (2012) A cytochrome b5-containing plastid-located fatty acid desaturase from *Chlamydomonas reinhardtii*. Eukaryot Cell **11:** 856–863